References

1. Rajewsky, K. 1990. Clonal selection and learning in the antibody system. *Nature 381:751.*
2. Goodnow, C. C. 1996. Balancing immunity and tolerance: deleting and tuning lymphocyte repertoires. *Proc. Natl. Acad. Sci. USA 93:2264.*
3. Karasuyama, H., A. Kudo, and F. Melchers. 1990. The proteins encoded by the VpreB and λ5 pre-B cell specific genes can associate with each other and with μ heavy chain. *J. Exp. Med. 172:969.*
4. Karasuyama, H., A. Rolink, Y. Shinkai, F. Young, F. W. Alt, and F. Melchers. 1994. The expression of VpreB/λ5 surrogate light chain in early bone marrow precursor B cells of normal and B cell-deficient mutant mice. *Cell 77:133.*
5. Melchers, F., A. Rolink, U. Grawunder, T. H. Winkler, H. Karasuyama, P. Ghia, and J. Andersson. 1995. Positive and negative selection events during B lymphopoiesis. *Curr. Opin. Immunol. 7:214.*
6. Karasuyama, H., A. Rolink, and F. Melchers. 1996. Surrogate light chain in B cell development. *Adv. Immunol. 63:1.*
7. Ling, N. R., I. C. M. MacLennan, and D. Y. Mason. 1987. B-cell and plasma cell antigens: new and previously defined clusters. In *Leucocyte Typing III.* A. J. McMichael, P. C. L. Beverley, S. Cobbold, M. J. Crumpton, W. Gilks, F. M. Gotch, N. Hogg, M. Horton, N. Ling, I. C. M. MacLennan, D. Y. Mason, C. Milstein, D. Spiegelhalter, and H. Waldmann, eds. Oxford Univ. Press, Oxford, p. 302.
8. Hunte, B. E., M. Capone, A. Zlotnik, D. Rennick, and T. A. Moore. 1998. Acquisition of CD24 expression by $Lin^{-}CD43^{+}B220^{low}ckit^{hi}$ cells coincides with commitment to the B cell lineage. *Eur. J. Immunol. 28:3850.*
9. Kokai, Y., Y. Ishii, and K. Kikuchi. 1986. Characterization of two distinct antigens expressed on either resting or activated human B cells as defined by monoclonal antibodies. *Clin. Exp. Immunol. 64:382.*
10. Kiyokawa, N., Y. Kokai, K. Ishimoto, H. Fujita, J. Fujimoto, and J. I. Hata. 1990. Characterization of the common acute lymphoblastic leukaemia antigen (CD10) as an activation molecule on mature human B cells. *Clin. Exp. Immunol. 79:322.*
11. Galibert, L., N. Burdin, B. de Saint-Vis, P. Garrone, C. Van Kooten, J. Banchereau, and F. Rousset. 1996. CD40 and B cell antigen receptor dual triggering of resting B lymphocytes turns on a partial germinal center phenotype. *J. Exp. Med. 183:77.*
12. Ingvarsson, S., K. Dahlenborg, R. Carlsson, and C. A. Borrebaeck. 1999. Coligation of CD44 on naive human tonsillar B cells induces progression towards a germinal center phenotype. *Int. Immunol. 11:739.*
13. Fischer, G. F., O. Majdic, S. Gadd, and W. Knapp. 1990. Signal transduction in lymphocytic and myeloid cells via CD24, a new member of phosphoinositol-anchored membrane molecules. *J. Immunol. 144:638.*
14. Lund-Johansen, F., J. Olweus, F. W. Symington, A. Arli, J. S. Thompson, R. Vilella, K. Skubitz, and V. Horejsi. 1993. Activation of human monocytes and granulocytes by monoclonal antibodies to glycosylphosphatidylinositol-anchored antigens. *Eur. J. Immunol. 23:2782.*
15. Kadmon, G., F. von Bohlen und Halbach, M. Schachner, and P. Altevogt. 1994. Differential, LFA-1-sensitive effects of antibodies to nectadrin, the heat-stable antigen, on B lymphoblast aggregation and signal transduction. *Biochem. Biophys. Res. Commun. 198:1209.*
16. Hough, M. R., M. S. Chappel, G. Sauvageau, F. Takei, R. Kay, and R. K. Humphries. 1996. Reduction of early B lymphocyte precursors in transgenic mice overexpressing the murine heat-stable antigen. *J. Immunol. 156:479.*
17. Chappel, M. S., M. R. Hough, A. Mittel, F. Takei, R. Kay, and R. K. Humphries. 1996. Cross-linking the murine heat-stable antigen induces apoptosis in B cell precursors and suppresses the anti-CD40-induced proliferation of mature resting B lymphocytes. *J. Exp. Med. 184:1638.*
18. Suzuki, T., N. Kiyokawa, T. Taguchi, T. Sekino, Y. U. Katagiri, and J. Fujimoto. 2001. CD24 induces apoptosis in human B cells via the GEM/rafts-mediated signaling system. *J. Immunol. 166:5567.*
19. Tsuganezawa, K., N. Kiyokawa, M. Matsuo, F. Kitamura, N. Toyama-Sorimachi, K. Kuida, J. Fujimoto, and H. Karasuyama. 1998. Flow cytometric diagnosis of the cell lineage and developmental stage of acute lymphoblastic leukemia by novel monoclonal antibodies specific to human preB cell receptor. *Blood 92:4317.*
20. Hirose, M., K. Minato, K. Tobinai, M. Ohira, T. Ise, S. Watanabe, M. Shimoyama, M. Taniwaki, and T. Abe. 1982. A novel pre-T cell line derived from acute lymphoblastic leukemia. *Gann 73:600.*
21. Yoshimura, T., M. Mayumi, T. Yorifuji, K. M. Kim, T. Heike, T. Miyanomae, K. Shinomiya, and H. Mikawa. 1987. Establishment of a common acute lymphoblastic leukemia cell line (LC4-1) and effects of phorbol myristate acetate (PMA) on the surface antigen expression of the cell line. *Am. J. Hematol. 26:47.*
22. Schneider, U., H. U. Schwenk, and G. Bornkamm. 1977. Characterization of EBV-genome negative "null" and "T" cell lines derived from children with acute lymphoblastic leukemia and leukemic transformed non-Hodgkin lymphoma. *Int. J. Cancer 19:621.*
23. Kiyokawa, N., E. K. Lee, D. Karunagaran, S.-Y. Lin, and M.-C. Hung. 1997. Mitosis-specific negative regulation of epidermal growth factor receptor, triggered by a decrease in ligand binding and dimerization, can be overcome by overexpression of receptor. *J. Biol. Chem. 272:18656.*
24. Henkart, P. A. 1996. ICE family proteases: mediators of all apoptotic cell death? *Immunity 4:195.*
25. Zarn, J. A., S. M. Zimmermann, M. K. Pass, R. Waibel, and R. A. Stahel. 1996. Association of CD24 with the kinase c-fgr in a small cell lung cancer cell line and with the kinase *lyn* in an erythroleukemia cell line. *Biochem. Biophys. Res. Commun. 225:384.*
26. Sammar, M., E. Gulbins, K. Hilbert, F. Lang, and P. Altevogt. 1997. Mouse CD24 as a signaling molecule for integrin-mediated cell binding: functional and physical association with *src*-kinases. *Biochem. Biophys. Res. Commun. 234:330.*
27. Horejsi, V., K. Drbal, M. Cebecauer, J. Cerny, T. Brdicka, P. Angelisova, and H. Stockinger. 1999. GPI-microdomains: a role in signalling via immunoreceptors. *Immunol. Today 20:356.*
28. Ilangumaran, S., H. T. He, and D. C. Hoessli. 2000. Microdomains in lymphocyte signalling: beyond GPI-anchored proteins. *Immunol. Today 21:2.*
29. Xia, Z., M. Dickens, J. Raingeaud, R. J. Davis, and M. E. Greenberg. 1995. Opposing effects of ERK and JNK-p38 MAP kinases on apoptosis. *Science 270:1326.*
30. Sugawara, T., T. Moriguchi, E. Nishida, and Y. Takahama. 1998. Differential roles of ERK and p38 MAP kinase pathways in positive and negative selection of T lymphocytes. *Immunity 9:565.*
31. Nagata, K., T. Nakamura, F. Kitamura, S. Kuramochi, S. Taki, K. S. Campbell, and H. Karasuyama. 1997. The Igα/Igβ heterodimer on μ-negative proB cells is competent for transducing signals to induce early B cell differentiation. *Immunity 7:559.*
32. Guan, Z., L. D. Baier, and A. R. Morrison. 1997. p38 mitogen-activated protein kinase down-regulates nitric oxide and up-regulates prostaglandin E_2 biosynthesis stimulated by interleukin-1β. *J. Biol. Chem. 272:8083.*
33. Guan, Z., S. Y. Buckman, A. P. Pentland, D. J. Templeton, and A. R. Morrison. 1998. Induction of cyclooxygenase-2 by the activated MEKK1→SEK1/MKK4→p38 mitogen-activated protein kinase pathway. *J. Biol. Chem. 273:12901.*
34. Brunet, A., and J. Pouyssegur. 1996. Identification of MAP kinase domains by redirecting stress signals into growth factor responses. *Science 272:1652.*
35. Zhang, C., R. A. Baumgartner, K. Yamada, and M. A. Beaven. 1997. Mitogen-activated protein (MAP) kinase regulates production of tumor necrosis factor-α and release of arachidonic acid in mast cells: indications of communication between p38 and p42 MAP kinases. *J. Biol. Chem. 272:13397.*
36. Pang, L., T. Sawada, S. J. Decker, and A. R. Saltiel. 1995. Inhibition of MAP kinase kinase blocks the differentiation of PC-12 cells induced by nerve growth factor. *J. Biol. Chem. 270:13585.*
37. Dudley, D. T., L. Pang, S. J. Decker, A. J. Bridges, and A. R. Saltiel. 1995. A synthetic inhibitor of the mitogen-activated protein kinase cascade. *Proc. Natl. Acad. Sci. USA 92:7686.*
38. Nagata, S. 1997. Apoptosis by death factor. *Cell 88:355.*
39. Kitamura, D., A. Kudo, S. Schaal, W. Muller, F. Melchers, and K. Rajewsky. 1992. A critical role of λ5 protein in B cell development. *Cell 69:823.*
40. Martensson, A., Y. Argon, F. Melchers, J. L. Dul, and I. L. Martensson. 1999. Partial block in B lymphocyte development at the transition into the pre-B cell receptor stage in Vpre-B1-deficient mice. *Int. Immunol. 11:453.*
41. Shimizu, T., C. Mundt, S. Licence, F. Melchers, and I. L. Martensson. 2002. VpreB1/VpreB2/λ5 triple-deficient mice show impaired B cell development but functional allelic exclusion of the IgH locus. *J. Immunol. 168:6286.*

British Journal of Haematology, 2003, 121, 94–96

SHORT REPORT

Anaplastic large cell lymphoma in Japanese children: retrospective analysis of 34 patients diagnosed at the National Research Institute for Child Health and Development

TETSUYA MORI,[1,2] NOBUTAKA KIYOKAWA,[1] HIROYUKI SHIMADA,[2] JUN MIYAUCHI[3] AND JUNICHIRO FUJIMOTO[1] [1]*Department of Developmental Biology, National Research Institute for Child Health and Development,* [2]*Department of Paediatrics, Keio University School of Medicine, and* [3]*Department of Pathology, National Centre for Child Health and Development, Tokyo, Japan*

Received 18 September 2002; accepted for publication 15 November 2002

Summary. This report presents a retrospective study of 34 Japanese children diagnosed at a single laboratory as having anaplastic large cell lymphoma (ALCL). Most of the pathological features of the Japanese ALCL children observed, such as anaplastic lymphoma kinase protein expression, in addition to most of the clinical characteristics and the outcomes of the patients, are very similar to those reported by European groups. To our knowledge, this is the first report describing the details of the clinicopathological features of Japanese ALCL patients. A further International study, including Japanese patients, might contribute to the establishment of an optimal treatment for paediatric ALCL.

Keywords: anaplastic large cell lymphoma, large cell lymphoma, CD30, anaplastic lymphoma kinase, paediatric cancer.

Anaplastic large cell lymphoma (ALCL) is a distinct clinicopathological entity of non-Hodgkin's lymphoma (Stein *et al*, 1985), which has been included in the recent World Health Organization (WHO) classification as a T-cell neoplasm (Jaffe *et al*, 2001). Because it is a relatively rare disease, the optimal treatment for childhood ALCL is yet to be determined. Most previous studies of childhood ALCL have been undertaken in populations with homogeneous racial backgrounds in European and North American centres (Brugieres *et al*, 1998; Mora *et al*, 2000; Seidemann *et al*, 2001; Alessandri *et al*, 2002; Williams *et al*, 2002). To our knowledge, there are few data on Japanese patients with ALCL (Kuze *et al*, 1996; Nakagawa *et al*, 1997). We report here the Japanese experience with regard to pathological and clinical characteristics of children with ALCL diagnosed by a single laboratory.

PATIENTS AND METHODS

A total of 34 patients with lymphoma were diagnosed as having ALCL in our laboratory. All but two of these patients were submitted for a diagnostic opinion between 1986 and 2001. In two patients, who presented before 1985, the original diagnosis had been Hodgkin's lymphoma. These patients were re-diagnosed as having ALCL after the later review of the original biopsy materials. Diagnosis of ALCL was based on morphological and immunological criteria defined by the new WHO classification. All diagnostic materials were reviewed, retrospectively, by the same pathologist. Medical records, including the clinical, treatment and outcome details, were collected from each treatment hospital retrospectively. Of the 34 patients, such information was available for 31. Overall survival rates and disease-free survival rates were estimated using the Kaplan–Meier method (Kaplan & Meier, 1958).

Correspondence: Tetsuya Mori, Department of Paediatrics, Keio University School of Medicine, 35 Shinanomachi, Shinjuku-ku, Tokyo 160–8582, Japan. E-mail: morite@sc.itc.keio.ac.jp

RESULTS

All cases were positive for CD30 and were classified as the ALCL common type (ALCL-CT) histological subgroup. Anaplastic lymphoma kinase (ALK) protein expression was found in 29 (88%) of 33 patients with p80 or ALK-1 antibodies. Granzyme-B was positive in 13 (62%) of 21 patients tested. Ten (43%) of 23 examined patients were classified as the T-cell phenotype (expression of CD3, CD43 or CD45RO) and the remaining 13 patients were classified as the null-cell phenotype.

Table I. Clinical characteristics and outcomes of patients.
(A) Clinical characteristics.

Characteristics	Patients Number	%
Age (median)	2–18 (11)	
Male:female	19:12	61%:39%
Stage (St Jude) I:II:III:IV	3:2:23:3	10%:6%:74%:10%
Adenopathy, any	30	97%
Peripheral	26	84%
Mediastinal	16	52%
Retroperitoneal	12	39%
Extranodal disease, any	21	68%
CNS disease	0	0%
Bone marrow	3	10%
Bone	6	19%
Skin/soft tissue	4	13%
Pleural effusion	7	23%
Splenomegaly	7	23%
Hepatomegaly	8	26%
Pericardial effusion	1	3%

(B) Outcomes and treatments.

	Total	~1994*	1995~*
Survived	23	13	10
Died	8	6	2
Relapse, progressive disease	9	6	3
Chemotherapy			
Prolonged (i.e. T-cell NHL type)	10	10	0
Short (i.e. B-cell NHL type)	21	9	12
Stem cell transplantation	6	4	2
after relapse	4	2	2
Radiation therapy	9	8	1
after relapse	5	4	1

*Year diagnosed.
Outcomes (data available = 31 patients). NHL, non-Hodgkin's lymphoma.

The clinical characteristics and outcomes of the 31 patients for whom data were available are summarized in Table I. The median age of the patients was 11 years, with a range between 2 and 18 years. The male:female ratio was 1·6:1. According to the St Jude staging system (Murphy, 1980), 26 (84%) of the 31 patients had advanced stage disease. Bone marrow involvement was present in three patients (10%), in whom the marrow involvement was scattered and scarce with <2% of lymphoma cells on smears. The central nervous system (CNS) was not affected in any patient. Lymphadenopathy was present in 30 (97%) of these patients. Extranodal involvement was observed in 21 (68%) of the patients; only one patient had exclusively extranodal disease. Four of the six patients with bone involvement had multiple bone disease.

Twenty-eight of 31 patients achieved complete remission (CR). One patient in the first CR died of cardiomyopathy 35 months after diagnosis. All three patients who failed to achieve CR died between 2 and 8 months after diagnosis. Six of the 28 CR patients relapsed between 3 and 25 months after diagnosis (median 8 months) and a second remission was achieved in four of the six. Two of these patients were still alive at the time of this report and were in the second and third remission, respectively, while the other two patients died of infection during chemotherapy in the second and fourth remission respectively. The remaining two patients who experienced relapse failed to achieve a second CR and died of their disease at 2–6 months after relapse.

In 21 of the 31 patients, short and intensive chemotherapy regimens were applied, as for B-cell lymphoma. In the other 10 patients, more prolonged chemotherapy derived from T-cell lymphoma regimens was applied. All of the 12 patients diagnosed since 1995 were treated with short chemotherapy regimens that were either similar to or identical to those previously reported by the Berlin–Frankfurt–Munster (BFM) group (Reiter *et al*, 1994). Local radiotherapy was used in nine patients. Autologous stem cell transplantation (auto-SCT) was performed in six patients, four of whom underwent auto-SCT after relapse. Only one of these patients was still in CR at the time of writing. Another patient relapsed after auto-SCT, after which she achieved and maintained a CR through treatment with conventional chemotherapy after the second relapse.

The median follow-up of these patients was 45 months (range between 2 and 223 months). Five-year overall and disease-free survival rates were 71·2% and 66·7% respectively (Fig 1). The 5 year disease-free survival rate of patients diagnosed in 1995 or later was 72·9%, whereas that of patients diagnosed before 1995 was 63·2%. This difference was not significant.

DISCUSSION

To our knowledge, this is the first report describing the clinicopathological features of Japanese patients with ALCL. One reason for the scarcity of data on Japanese children with ALCL may be as a result of the lack of a sufficient

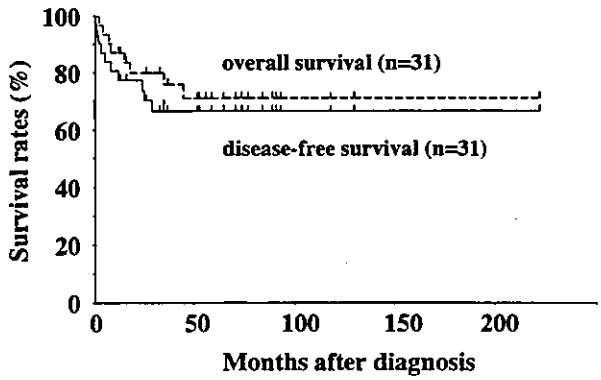

Fig 1. Survival curves. The Kaplan–Meier estimate of overall and disease-free survival rates of the 31 patients enrolled in this study. The 5-year disease-free survival was 66·7% and the 5-year overall survival was 71·2%; n = number of patients.

nationwide clinical study system for relatively rare childhood cancers in Japan. Most of the pathological and clinical features of the Japanese ALCL children in the present study are similar to those in previous reports (Brugieres *et al*, 1998; Mora *et al*, 2000; Seidemann *et al*, 2001; Alessandri *et al*, 2002; Williams *et al*, 2002). Although the outcomes in the present study may be less informative because most of these children were treated according to various regimens selected in hospitals at which the patient presented, the survival rates, especially those of patients diagnosed in 1995 or after, are comparable to those of recent European studies.

Most of the diagnostic materials in the present study had been sent for a diagnostic opinion to our laboratory from the hospital at which the patient originally presented. Because of this, the series of ALCL patients reported here may be influenced by a selective bias. It should be noted that it is not certain that all ALCL patients diagnosed in individual hospitals were enrolled in this study, as the only diagnostic materials used for this study were those sent to our laboratory for a diagnostic opinion.

Our data suggest that there are no significant ethnic differences in the pathological and clinical characteristics observed between Japanese ALCL children and those in the European reports. One reason why an optimal treatment for paediatric ALCL has yet to be determined is the relatively rarity of ALCL. A further International study, including Japanese patients, may contribute to the establishment of an optimal treatment for paediatric ALCL.

ACKNOWLEDGMENTS

The authors thank the clinicians and the pathologists at the following institutions who contributed their ALCL patients to this study: N. Taguchi and M. Kumagai, National Children's Hospital (Tokyo); T. Kaneko and J. Takayama, Metropolitan Kiyose Children's Hospital (Tokyo); K. Ishimoto, Juntendo University (Tokyo); K. Nishihira, Kanagawa Children's Medical Center (Yokohama); K. Sugita, Dokkyo University (Tochigi); K. Hiraoka, National Shimonoseki Hospital (Shimonoseki); T. Fujisawa, Nihon University (Tokyo); M. Maeda, Nippon Medical School (Tokyo); Y. Kobayashi, Osaka City General Hospital (Osaka); T. Hattori, Teikyo University (Tokyo); H. Yabe, Tokai University (Isehara); K. Tabuchi, Tokyo University (Tokyo); H. Kato, Tokyo Women's Medical University (Tokyo); I. Tsukimoto, Toho University (Tokyo); and J. Hata, Keio University (Tokyo).

REFERENCES

Alessandri, A.J., Pritchard, S.L., Schultz, K.R. & Massing, B.G. (2002) A population-based study of pediatric anaplastic large cell lymphoma. *Cancer*, 94, 1830–1835.

Brugieres, L., Deley, M.C., Pacquement, H., Meguerian-Bedoyan, Z., Terrier-Lacombe, M.J., Robert, A., Pondarre, C., Leverger, G., Devalck, C., Rodary, C., Delsol, G. & Hartmann, O. (1998) CD30(+) anaplastic large-cell lymphoma in children: analysis of 82 patients enrolled in two consecutive studies of the French Society of Pediatric Oncology. *Blood*, 92, 3591–3598.

Jaffe, E.S., Harris, N.L., Stein, H. & Vardiman, J.W. (2001) *World Health Organization classification of tumors, Pathology and genetics of tumors of haematopoietic and lymphoid tissues* IARC Press, Lyon.

Kaplan, E.L. & Meier, P. (1958) Nonparametric estimation from incomplete observations. *Journal of American Statistical Association*, 53, 457–481.

Kuze, T., Nakamura, N., Hashimoto, Y., Abe, M. & Wakasa, H. (1996) Clinicopathological, immunological and genetic studies of CD30+ anaplastic large cell lymphoma of B-cell type: association with Epstein–Barr virus in a Japanese population. *Journal of Pathology*, 180, 236–242.

Mora, J., Filippa, D.A., Thaler, H.T., Polyak, T., Cranor, M.L. & Wollner, N. (2000) Large cell non-Hodgkin lymphoma of childhood: analysis of 78 consecutive patients enrolled in 2 consecutive protocols at the Memorial Sloan–Kettering Cancer Center. *Cancer*, 88, 186–197.

Murphy, S.B. (1980) Classification, staging and end results of treatment of childhood non-Hodgkin's lymphomas: dissimilarities from lymphomas in adults. *Seminars in Oncology*, 7, 332–339.

Nakagawa, A., Nakamura, S., Ito, M., Shiota, M., Mori, S. & Suchi, T. (1997) CD30-positive anaplastic large cell lymphoma in childhood: expression of p80npm/alk and absence of Epstein–Barr virus. *Modern Pathology*, 10, 210–215.

Reiter, A., Schrappe, M., Tiemann, M., Parwaresch, R., Zimmermann, M., Yakisan, E., Dopfer, R., Bucsky, P., Mann, G., Gadner, H. & Riehm, H. (1994) Successful treatment strategy for Ki-1 anaplastic large-cell lymphoma of childhood: a prospective analysis of 62 patients enrolled in three consecutive Berlin–Frankfurt–Munster group studies. *Journal of Clinical Oncology*, 12, 899–908.

Seidemann, K., Tiemann, M., Schrappe, M., Yakisan, E., Simonitsch, I., Janka-Schaub, G., Dorffel, W., Zimmermann, M., Mann, G., Gadner, H., Parwaresch, R., Riehm, H. & Reiter, A. (2001) Short-pulse B-non-Hodgkin lymphoma-type chemotherapy is efficacious treatment for pediatric anaplastic large cell lymphoma: a report of the Berlin–Frankfurt–Munster Group Trial NHL-BFM 90. *Blood*, 97, 3699–3706.

Stein, H., Mason, D.Y., Gerdes, J., O'Connor, N., Wainscoat, J., Pallesen, G., Gatter, K., Falini, B., Delsol, G., Lemke, H., Schwarting, R. & Lennert, K. (1985) The expression of the Hodgkin's disease associated antigen Ki-1 in reactive and neoplastic lymphoid tissue: evidence that Reed–Sternberg cells and histiocytic malignancies are derived from activated lymphoid cells. *Blood*, 66, 848–858.

Williams, D.M., Hobson, R., Imeson, J., Gerrard, M., McCarthy, K. & Pinkerton, C.R. (2002) Anaplastic large cell lymphoma in childhood: analysis of 72 patients treated on the United Kingdom Children's Cancer Study Group chemotherapy regimens. *British Journal of Haematology*, 117, 812–820.

Leukemia (2003) 17, 1164–1174

www.nature.com/leu

Costimulatory signals distinctively affect CD20- and B-cell-antigen-receptor-mediated apoptosis in Burkitt's lymphoma/leukemia cells

K Mimori[1,2], N Kiyokawa[1], T Taguchi[1], T Suzuki[1], T Sekino[1], H Nakajima[1], M Saito[1], YU Katagiri[1], K Isoyama[2], K Yamada[2], Y Matsuo[3] and J Fujimoto[1]

[1]*Department of Developmental Biology, National Research Institute for Child Health and Development, Tokyo, Japan;* [2]*Department of Pediatrics, Showa University Fujigaoka Hospital, Yokohama, Kanagawa, Japan; and* [3]*Fujisaki Cell Center, Hayashibara Biochemical Labs Inc., Okayama, Japan*

CD20 is a B-cell differentiation antigen and known to induce apoptosis in Burkitt's lymphoma/leukemia (BL) cells upon antibody-mediated crosslinking. We examined the biological effect of CD20 crosslinking on BL cell lines and observed that apoptosis induction is accompanied by activation of multiple caspases, including caspase-8, -9, -3, -2, and -7. Further investigation revealed a clear synergism between apoptosis mediated by CD20 and by B-cell antigen receptor (BCR). Examination of the effect of simultaneous crosslinking of other cell surface molecules with crosslinking of CD20 or BCR on apoptosis induction showed that these molecules had either a synergistic or inhibitory effect on induction of apoptosis. It is worth noting that some molecules had a different effect on CD20- and BCR-mediated apoptosis. Simultaneous crosslinking of the molecules CD10, CD22, CD72, and CD80 inhibited BCR-mediated apoptosis, but enhanced CD20-mediated apoptosis. Further studies revealed that regulation of CD20-induced apoptosis by other costimulatory molecules is achieved by modification of caspase activation. CD20-mediated apoptosis in BL cells may provide not only a model for understanding the mechanism regulating clonal selection of B cells but a new therapeutic strategy for BL patients.
Leukemia (2003) **17**, 1164–1174. doi:10.1038/sj.leu.2402936
Keywords: CD20; BCR; Apoptosis; Burkitt's cells; caspase

Introduction

In the process of maturation, B cells proceed through multiple developmental stages that determine whether they will survive or die, changing their phenotypes in a developmental stage-dependent manner.[1–3] There is no doubt that B-cell antigen receptor (BCR) is crucial for the signaling that determines the fate of B cells. In addition to BCR, however, a number of B-cell differentiation antigens have been found to mediate signal transduction that leads to proliferation and differentiation upon binding with their specific ligands and to cooperatively regulate the process of B-cell differentiation.[4–6] Thus, identifying the stimuli mediated by these surface molecules should provide an approach to understanding the molecular basis of B-cell development.

CD20 is a B-cell antigen that is expressed from the late pre-B-cell stage until being lost just prior to terminal differentiation into plasma cells, and it is thought to have a regulatory function in B-cell proliferation and differentiation.[7] A number of studies have indicated that CD20 mediates intracellular signals.[8–10] For example, CD20 is closely associated with Src-family protein tyrosine kinases (PTKs) Lyn, Fyn, and Lck, and induces activation of these PTKs upon crosslinking mediated by specific antibodies (Abs).[9] Additional signaling pathways, involving activation of PLC-γ1 and PLC-γ2 or activation of the mitogen-activated protein kinases (MAPKs), have been describec previously.[8,10] In addition, evidence suggests that CD20 may also be involved in the control of free calcium concentration by regulating both calcium influx and mobilization of calcium from intracellular stores.[11]

More recently, crosslinking of CD20 has been shown to induce apoptosis in B cells.[12] Clinical administration of IDEC-C28, a mouse–human chimeric Ab against CD20, can induce remission of low-grade B-lineage lymphomas.[13] It was originally suggested that the main mechanisms of this action are complement-mediated and Ab-dependent cell-mediated cytotoxicity,[14] but a recent study has demonstrated that Ab-mediated crosslinking of CD20 induces apoptosis in B-lineage lymphoma cell lines, including Burkitt's lymphoma (BL) cells.[10]

The fact that CD20-mediated apoptosis is inhibited either by a selective inhibitor of the Src-family PTK, PP2, or by EGTA and BAPTA, which block changes in cytoplasmic Ca^{2+}, has suggested the involvement of CD20-mediated signaling events in the apoptotic process.[15,16] Although it is unclear how the CD20-mediated signals initiate events further downstream that lead to the apoptotic process, involvement of the rapid downregulation of c-myc and upregulation of Bax, a Bcl-2-family protein, followed by activation of caspase-3 has been reported.[10,15,16] BL cells are also known to be induced to undergo apoptosis by activation of BCR.[17] The fact that both apoptotic processes share similar intracellular events, such as activation of MAPKs, similar changes in the expression of c-myc and Bax, and caspase-3 activation, has suggested a close correlation between CD20- and BCR-mediated apoptosis.[10] Both pathways are probably mediated in part by the same signal-transducing molecules, but the details are for the most part unknown.

In the present study, we further investigated the details of the intracellular events that occur during the process of CD20-mediated apoptosis. Our findings extend the observations of others and indicate involvement of activation of multiple caspase cascades in CD20-mediated apoptosis and show that costimulatory signals by a number of B-cell surface molecules modulate the CD20-mediated apoptotic process by affecting the caspase cascade. Although clear synergism between CD20 and BCR crosslinking on the apoptosis-inducing effect was observed, these two apoptotic signaling pathways are distinctly regulated by other costimulatory signals.

Materials and methods

Cells

BL-derived cell lines, Daudi, Ramos, Raji, P32/ISH (Japanese *Cancer Research* Resources Bank, Tokyo, Japan), CA-46

Correspondence: Dr J Fujimoto, Department of Developmental Biology, National Research Institute for Child Health and Development, 3-35-31, Taishido, Setagaya-ku, Tokyo 154-8567, Japan. Fax: +81 3 3487 9669
Received 4 April 2002; accepted 10 February 2003

(Dainippon Pharmacology Co., Osaka, Japan), EB-3, and Namalwa (Institute for Fermentation, Osaka, Japan) were used. An acute lymphoblastic leukemia L3 type (ALL-L3)-derived cell line BALM-18[18] was also used. Since ALL-L3 is thought to be the leukemic form of BL and has been designated as Burkitt leukemia in the new WHO classification of tumors of hematopoietic and lymphoid tissues,[19] we include ALL-L3-derived cell lines in BL-derived cell lines in this paper for convenience. Cells were cultured in RPMI1640 supplemented with 10% fetal calf serum at 37°C in a humidified 5% CO_2 atmosphere.

Reagents

The mouse monoclonal (m)Abs used for immunofluorescence study were: anti-CD20, anti-CD22, anti-CD32, anti-CD38, anti-CD40, anti-CD48, anti-CD70, anti-CD72, anti-CD80, anti-CD81, anti-CD95, and anti-CD124 from Beckman/Coulter Inc. (Westbrook, MA, USA); anti-CD55 and anti-CD59 from Pharmingen (San Diego, CA, USA); anti-CD19, anti-CD45, and anti-μ heavy chain from American Type Culture Collection (Rockville, MD, USA). Anti-CD10[20] and anti-CD24 (L30)[21] were also used. The mouse mAbs used for immunobiochemical study in this paper were: anti-caspase-2, anti-caspase-3, and anti-caspase-7 from Transduction Laboratories (Lexington, KY, USA); anti-PARP from Biomol Research Laboratories, Inc. (Plymouth Meeting, PA, USA); anti-β-actin from Seikagaku Co. (Tokyo, Japan). The rabbit polyclonal Abs used were: anti-caspase-8 from Santa Cruz Biotechnology (Santa Cruz, CA, USA); anti-caspase-9 and anti-Bid from New England Biolabs, Inc. (Bevely, MA, USA). Secondary Abs, including fluorescein- and enzyme-conjugated Abs were purchased from either Jackson Laboratory, Inc. or Molecular Probes (Eugene, OR, USA). Biotinylation of mAb was performed as described previously.[20] Conjugation of Alexa Fluor® 488 to anti-CD20 mAb was performed by using Alexa Fluor® 488 Monoclonal Antibody Labeling Kit (Molecular Probes) according to the manufacturer's protocol. Conjugation of Abs to polystyrene beads was performed as described previously.[22] To crosslink cell surface antigens, cells were cultured in the presence of Abs as indicated. In these cases, Abs were dialyzed in PBS prior to addition to culture to remove additives. All chemical reagents were obtained from Sigma-Aldrich Fine Chemicals (St Louis, MO, USA), unless otherwise indicated. The peptide inhibitors of caspase used in this study were: z-Tyr-Val-Ala-Asp-fluoromethyl ketone (z-YVAD-fmk, specific for caspase-1), z-Asp-Glu-Val-Asp (DEVD)-fmk (for caspase-3), z-Ile-Glu-Thr-Asp (IETD)-fmk (for caspase-8), z-Leu-Glu-His-Asp (LEHD)-fmk (for caspase-9), and z-Val-Ala-Asp (VAD)-fmk (for a broad spectrum of caspases) from Calbiochem-Novabiochem Co. (San Diego, CA, USA).

Immunofluorescence study and detection of apoptosis

To test the expression of cell surface antigens, cells were stained with FITC-labeled mAbs and analyzed by flow cytometry (EPICS-XL, Beckman/Coulter) as described previously.[20] To quantitate the incidence of apoptotic cells, cells were stained with FITC-labeled annexin-V by using a MEBCYTO®-Apoptosis Kit (Medical & Biological Laboratories, Co., LTD., MBL, Nagoya, Japan) and then analyzed by flow cytometry according to the manufacturer's protocol. Experiments were performed in triplicate, and the means $\pm$ s.d.s of the cells that bound annexin-V are shown. Caspase-3 activity was assessed with a PhiPhiLUX™ G1D2 kit (MBL) and analyzed by flow cytometry according to the manufacturer's protocol. To observe the extent of CD20 clustering on the cell surface, cells were stained with Alexa Fluor® 488-conjugated anti-CD20 mAb and examined by confocal microscopy (Fluoview FV500, Olympus, Co., Tokyo, Japan) using the appropriate filter set as described previously.[22]

Immunoblotting

A 50 μg quantity of each whole-cell lysate was electrophoretically separated on an SDS-polyacrylamide gel and transferred to a nitrocellulose membrane by a semidry transblot system (Bio-Rad Laboratories, Hercules, CA, USA). Immunoblotting was performed as described previously.[22]

Results

Establishment of cell line BALM-24

Peripheral blood mononuclear cells obtained from a 46-year-old female patient with ALL-L3 at diagnosis were cultured as described previously.[18] At the initiation of the culture, a mouse bone marrow stroma cell line MS-5 cells[23] were used as feeder cells. The cells began to proliferate 3 weeks after and adapted to growth in medium without feeder cells. When established, the cell line was designated BALM-24. Cytogenetic analysis of BALM-24 cells showed the t(8; 14)(q24.1; q32) chromosomal abnormality, which is highly associated with ALL-L3 and BL. Additional chromosomal abnormalities +add(1)(p?13), del(4)(q12), -13, -20, and +mar1 were observed.

Activation of caspases in the course of CD20-mediated apoptosis

First, we tested whether crosslinking of CD20 induces apoptosis in BL cells by using the newly established cell line BALM-24, which expresses CD20 (Figure 1). When BALM-24 cells were exposed to anti-CD20 mAb in the presence of secondary rabbit polyclonal anti-mouse Ig Ab for 24 h, more than 60% of the cells appeared to be annexin-V bound, indicating significant apoptosis induction (Figures 2a and 3a). When we tested anti-CD20 mAb immobilized on polystyrene beads and a combination of biotinylated anti-CD20 mAb and avidin, we obtained identical results (data not shown).

Since a number of studies have indicated that caspases are essential effector molecules in the apoptotic process in various cell systems,[24] we investigated whether they are activated during the apoptotic process induced by CD20 crosslinking in BALM-24 cells. When the cell lysates prepared from CD20-crosslinked BALM-24 cells, the levels of caspase proenzyme proteins, including those of caspase-8, -9, -3, -2, and -7, decreased markedly (Figure 2b) in parallel with the appearance of annexin-V-bound cells (Figure 2a), indicating cleavage of the proenzymes of these caspases. Even the p20 cleaved fragment of caspase-8 was observed after CD20 crosslinking in BALM-24 cells (Figure 2b). Immunoblot analysis also revealed cleavage of Bid, an apoptosis-related Bcl-2 family protein, and PARP, a substrate of caspases, during the course of apoptosis mediated by CD20 crosslinking in BALM-24 cells (Figure 2b). No significant change was observed in the protein level of β-actin, indicating that the amounts of protein loaded onto each lane were comparable (Figure 2b). We also tested the activity of

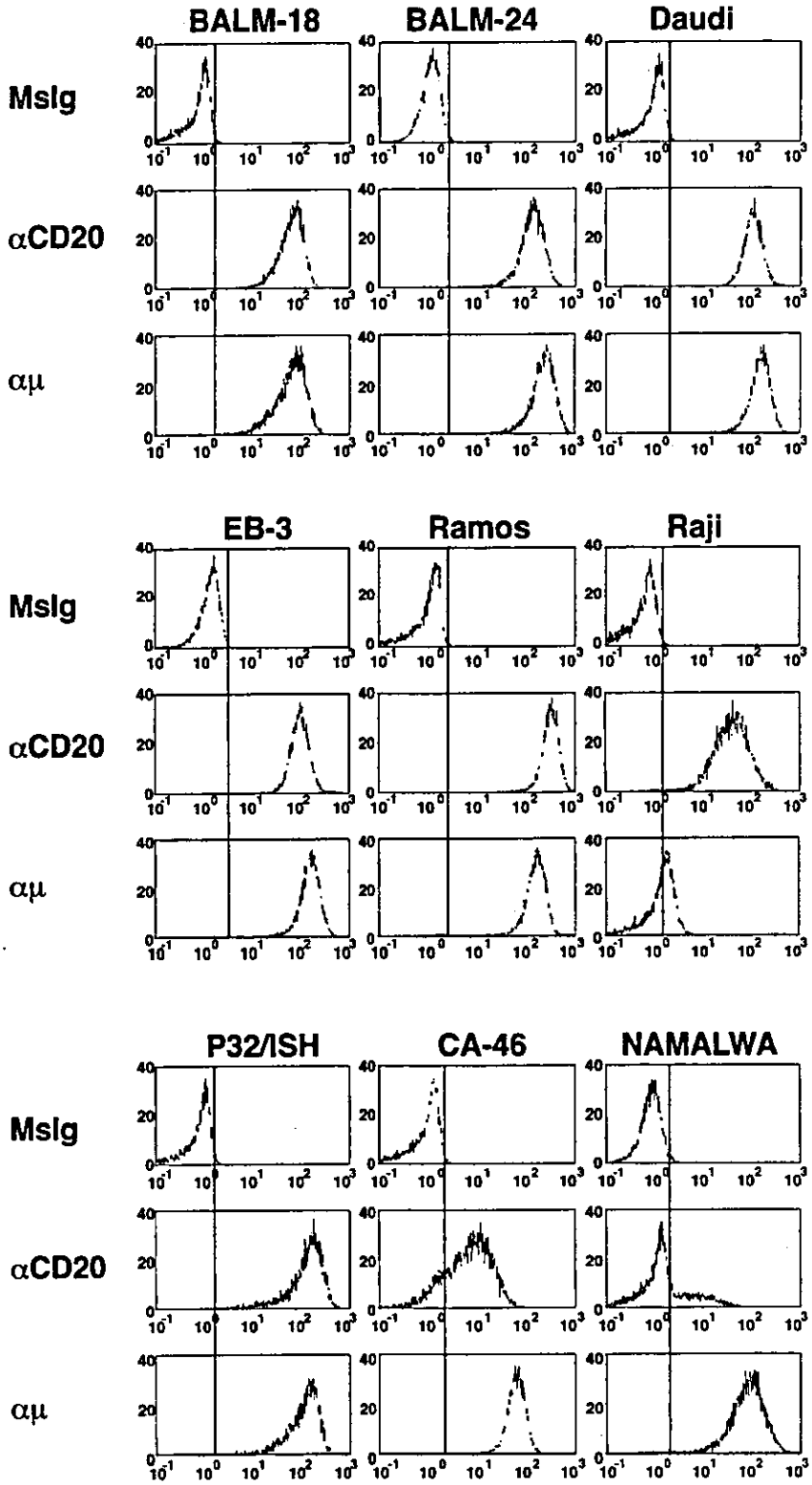

Figure 1 Expression of CD20- and B-cell antigen receptor in Burkitt's lymphoma/leukemia (BL) cells. The nine BL cell lines indicated were stained with FITC-labeled specific mAbs antibodies against CD20 and μ heavy chain, respectively, and analyzed by flow cytometry. The histograms obtained have been displayed with that of the negative control (cells stained with isotype-matched control mouse immunoglobulin, MsIg). *X*-axis, fluorescence intensity; *Y*-axis, relative cell number.

caspase-3 in individual cells by PhiPhiLux^{TM} G1D2. As shown in Figure 2c, a significant increase in fluorescence activity was observed in more than 60% of BALM-24 cells after CD20 crosslinking, indicating the activation of caspase-3 in these cells.

We then examined the enzymatic activity of caspase-3 by colorimetric assay in BALM-24 cells induced by CD20 cross-linking and exposed to the specific tetrapeptide substrate DEVD-*p*NA. As shown in Figure 4a, a significant elevation of DEVD-

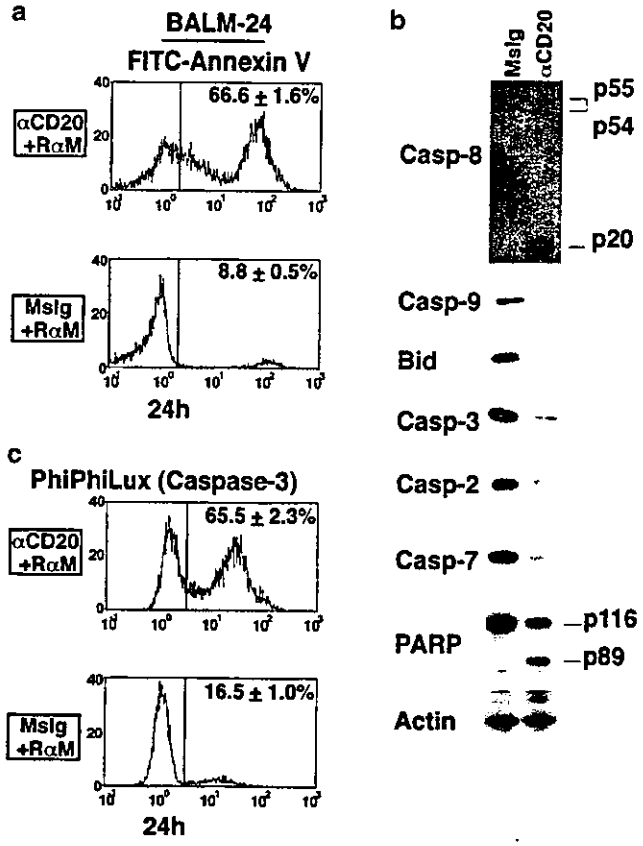

Figure 2 Activation of multiple caspases in the course of CD20-mediated apoptosis in BALM-24 cells. (a) BALM-24 cells (2.5×10^5 cells in 500 μl of medium) were exposed to either anti-CD20 monoclonal antibody (mAb) (αCD20, upper panel, 5 μg/ml) or isotype-matched control mouse immunoglobulin (MsIg, lower panel, 5 μg/ml) in the presence of secondary rabbit anti-mouse Ig Ab (RαM, 5 μg/ml) for 24 h. Apoptotic cells were detected by staining with FITC-conjugated annexin-V and analyzed by flow cytometry. The histograms obtained from each experiment are shown as in Figure 1. (b) Cell lysates were prepared from BALM-24 cells exposed to either αCD20 mAb (right lane) or MsIg (left lane) immobilized on polystyrene beads for 24 h and analyzed by immunoblotting with the Abs indicated. (c) Caspase-3 activity in the same sample preparation as in (A) was examined by using PhiPhiLux™ GiD2 and analyzed by flow cytometry.

*p*NA cleavage activity was detected in the cell lysate of CD20-crosslinked BALM-24 cells in parallel with the appearance of annexin-V-bound cells (Figure 2a). The elevation of this activity was highly consistent with the cleavage of the caspase-3 proenzyme detected by immunoblotting (Figure 2b) as well as the PhiPhiLux™ G1D2 cleavage activity (Figure 2c) mentioned above.

To further examine the involvement of activation of the caspase cascade in the process of CD20-mediated apoptosis, we examined the effect of peptide inhibitors of the caspases. When BALM-24 cells pretreated with z-VAD-fmk (a tripeptide inhibitor of a broad range of caspases) were incubated with a combination of anti-CD20 Ab and secondary anti-mouse Ab, the number of annexin-V-positive cells was significantly reduced compared with cells not exposed to z-VAD-fmk (Figure 4b). When we tested the effect of z-IETD-fmk (a tetrapeptide inhibitor of caspase-8), z-LEHD-fmk (a tetrapeptide inhibitor of caspase-9), and z-DEVD-fmk (a tetrapeptide inhibitor of caspase-3), a weak reduction in annexin-V-positive cells after CD20 crosslining was observed (Figure 4b), but it was no greater than observed with

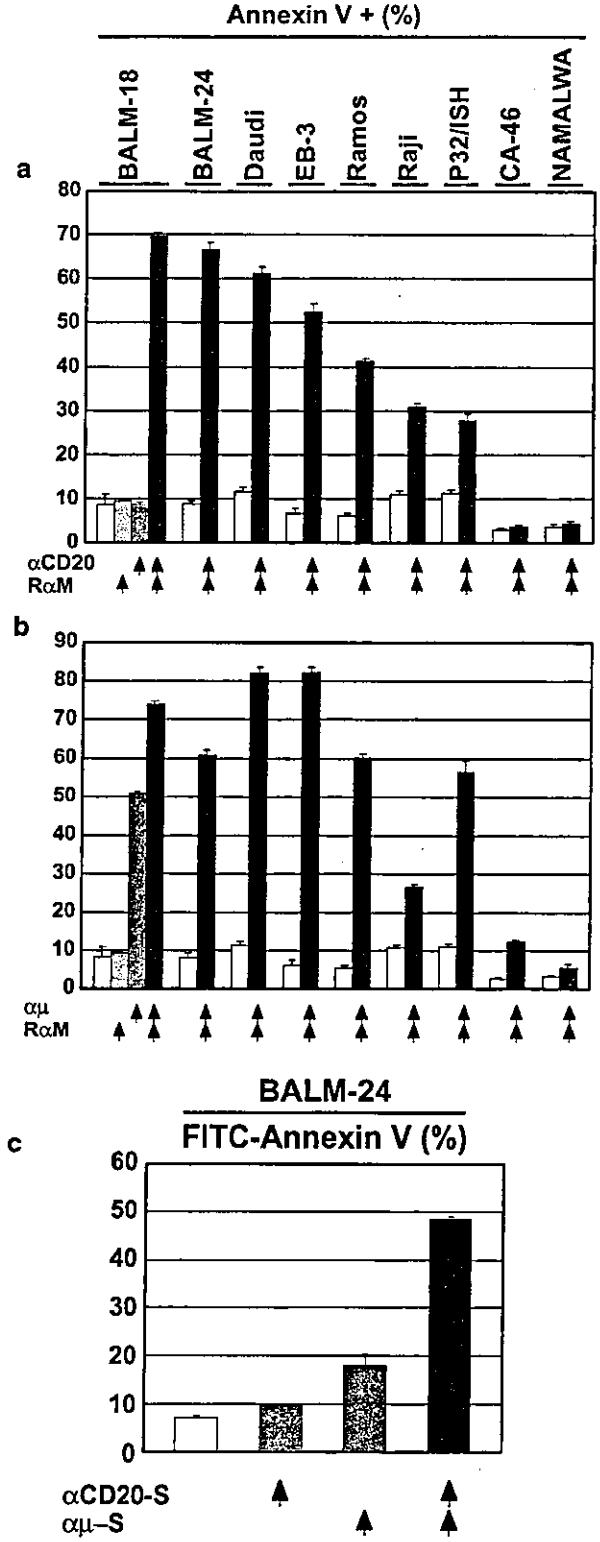

Figure 3 Apoptosis induction in Burkitt's lymphoma/leukemia (BL) cells mediated by crosslinking of CD20 and B-cell antigen receptor. The nine BL cell lines indicated were exposed to either (a) anti-CD20 monoclonal antibody (mAb) (αCD20, 5 μg/ml) or (b) anti-μ heavy-chain mAb (αμ, 5 μg/ml) in the presence of secondary rabbit anti-mouse Ig Ab (RαM, 5 μg/ml) for 24 h. Apoptotic cells were detected by annexin-V assay as in Figure 2a. (c) BALM-24 cells exposed and unexposed to a suboptimal dose of αCD20 mAb (αCD20-S, 0.5 μg/ml) (columns 2 and 4) and αμ mAb (αμ-S, 0.1 μg/ml) (columns 3 and 4) for 24 h were examined as in Figure 2a.

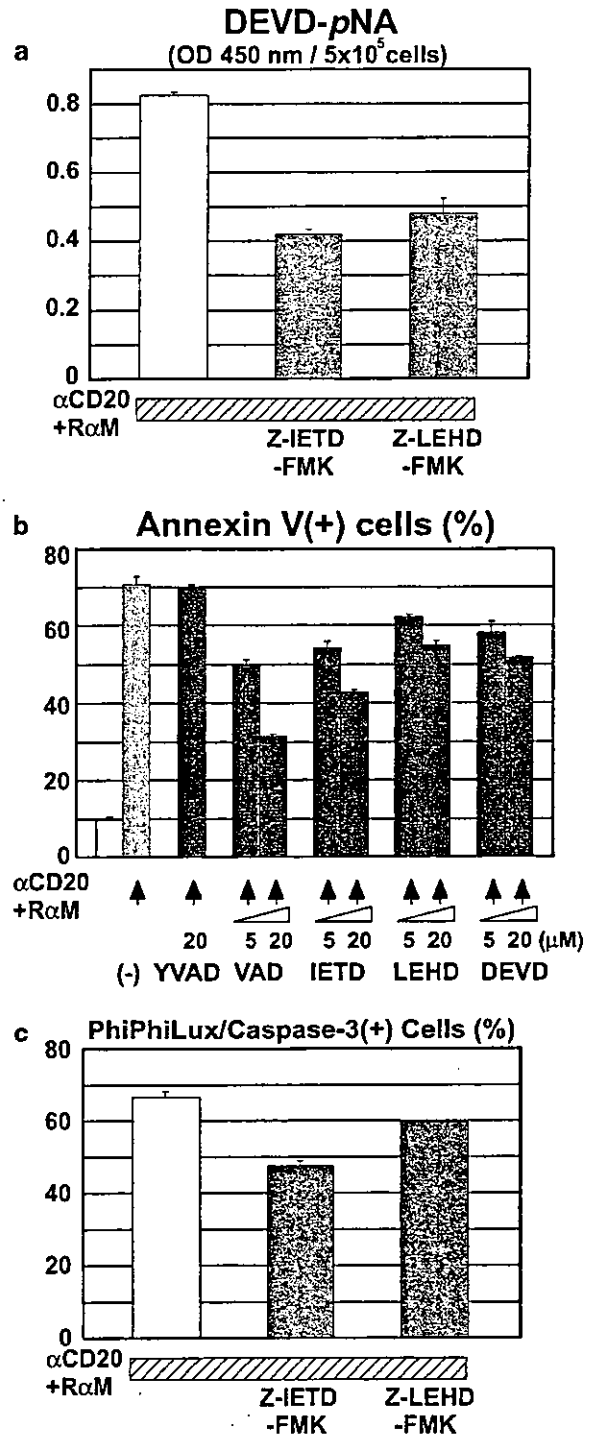

Figure 4 Effect of caspase inhibitors on CD20-induced apoptosis. (a) After 1-h pre-incubation with the peptide inhibitors of caspases indicated (20 μM each), BALM-24 cells were exposed to a combination of anti-CD20 monoclonal antibody (mAb) (αCD20, 5 μg/ml) and secondary rabbit anti-mouse Ig Ab (RαM, 5 μg/ml) for 24 h, and the subsequent caspase-3 activity was measured by colorimetric assay with the specific peptide substrate DEVD-*p*NA. (b) After cell preparation as in (a), the subsequent incidence of apoptotic cells was determined as in Figure 2a. (c) After cell preparation as in (a), individual cells were examined for caspase-3 activation by flow cytometry using PhiPhiLux™ GiD2. IETD for caspase-8; LEHD for caspase-9; YVAD for caspase-1; VAD for a broad spectrum of caspases; DEVD for caspase-3.

z-VAD-fmk. By contrast, pretreatment with z-YVAD-fmk (tetrapeptide inhibitor of caspase-1-like protease) did not cause any reduction in the number of apoptotic cells evaluated by annexin-V binding (Figure 4b), indicating that the above peptide inhibitors specifically inhibited of CD20-mediated apoptosis of BALM-24 cells. The evidence that this apoptotic process is inhibited by specific peptide inhibitors of caspases further indicates that the activation of the caspase cascade participates in the induction of apoptosis after CD20 crosslinking.

Caspases themselves have been shown to form a regulatory cascade that transduces apoptotic signals.[25] To clarify the cascade of caspases that is activated during CD20-mediated apoptosis in BALM-24 cells, we examined the effect of peptide inhibitors on the activation of caspase-3 induced by CD20 crosslinking. Evaluation based on DEVD-*p*NA cleavage activity measured by colorimetric assay showed that both z-IETD-fmk and LEHD-fmk significantly inhibited the activation of caspase-3 (Figure 4a), indicating that inhibition of caspase-8 or -9 leads to reduction of caspase-3 activation. Assessment with PhiPhiLux™ G1D2 further indicated that both z-IETD-fmk and LEHD-fmk reduced the number of cells in which caspase-3 was activated after CD20 crosslinking (Figure 4c). These findings indicate that both caspase-8 and -9 are located upstream of caspase-3 in the cascade. It should be noted that inhibition of caspase-8 was more effective than inhibition of caspase-9 in inhibiting caspase-3 activation (Figure 4a and c).

Crosslinking of CD20 and that of BCR synergisticcally affect apoptosis induction in BL cells

Next, we compared the apoptosis-inducing effect of CD20 crosslinking in different BL cell lines. Testing for cell surface expression of CD20 in various BL cell lines showed that most of the lines expressed CD20 (Figure 1). As shown in Figure 1, flow-cytometric analysis revealed high levels of expression of CD20 in seven cell lines; BALM-18, BALM-24, Daudi, EB-3, Ramos, Raji, and P32/ISH. By contrast, CA-46 and NAMALWA cells exhibited a lower level and faint expression, respectively, of CD20 (Figure 1). As shown in Figure 3a, annexin-V-binding assay revealed that the magnitude of apoptosis induction after CD20 crosslinking varied considerably among the BL lines and that it is not necessarily correlated with the level of expression of CD20. For example, in spite of comparable high levels of expression of CD20 in BALM-18 and P32/ISH cell lines, the incidence of apoptosis induction was approximately 70 and 30%, respectively (Figures 1 and 3a). On the other hand, although CA-46 cells express easily recognizable levels of CD20 (Figure 1), crosslinking of CD20 failed to induce apoptosis in these cells at all (Figure 3a).

Since crosslinking of BCR has also been reported to induce apoptosis in BL cells,[17] we examined the correlation between CD20 crosslinking and that of BCR on the apoptosis-inducing effect. As shown in Figure 1, flow cytometric analysis revealed high levels of expression of BCR on all BL lines tested, with the exception of Raji cells, which express only low amounts of BCR on the cell surface. When these BL lines were examined by annexin-V-binding assay, most of the lines expressing high levels of BCR showed a higher incidence of apoptosis induction after BCR crosslinking (Figure 3b). Interestingly, however, two lines, CA-46 and NAMALWA, which exhibited low sensitivity to CD20-mediated apoptosis, showed no significant induction of apoptosis after crosslinking of BCR either (Figure 3a and b).

We next examined crosslinking of BCR and that of CD20 for synergism in inducing of apoptosis. Since both anti-μ heavy-

chain mAb and anti-CD20 mAb effectively induce apoptosis in BALM-24 cells (Figure 3a and b), we employed suboptimal doses of these mAbs to be able to observe synergism clearly. When both mAbs were mixed under suboptimal conditions, clear synergism was observed between crosslinking of CD20 and that of BCR on apoptosis induction in BALM-24 cells (Figure 3c).

Effect of co-crosslinking of other cell surface molecules on CD20- and BCR-mediated apoptosis

BALM-24 cells express various B-cell differentiation antigens on their surface, as shown in Figure 5. We therefore investigated the effect of co-crosslinking of various cell surface molecules on both CD20- and BCR-mediated apoptosis. The cell surface molecules could be classified into several groups according to their effects. As shown in Figure 6, the GPI-anchored proteins, CD48, CD55, CD59, and CD24, clearly enhanced both CD20- and BCR-mediated apoptosis upon simultaneous crosslinking, and other molecules, CD38 (bifunctional ectoenzyme), CD19/CD81 (stimulatory coreceptor of BCR), CD45 (protein tyrosine phosphatase), and CD70 (CD27 ligand), also enhanced induction of apoptosis mediated by both CD20 and BCR upon simultaneous crosslinking (Figure 6). It should be noted that most of these molecules induced a low incidence of apoptosis by themselves, but that no induction of apoptosis was observed by CD81 or CD45 alone. By contrast, stimulation of the inhibitory coreceptors of BCR, such as CD32, CD40, and CD124 (IL-4 receptor), which inhibit BCR-mediated apoptosis (Figure 7c), also inhibited CD20-mediated apoptosis (Figure 7b). Interestingly, other molecules that significantly inhibited BCR-mediated apoptosis, CD80, CD10, CD22, and CD72 (Figure 7c), enhanced CD20-mediated apoptosis upon simultaneous crosslinking (Figure 7c). Co-crosslinking of CD95 (Fas) had no effect on either CD20- or BCR-mediated apoptosis in BALM-24 cells.

Since it was possible that the modulatory effect of other molecules varies significantly between cell lines, we similarly examined one additional cell line, P32/ISH, in which CD20 induces a low level of apoptosis. As shown in Figures 1 and 5, flow-cytometric analysis revealed that the pattern of expression of B-cell differentiation antigens by P32/ISH was similar to that of BALM-24 cells, with some exceptions, including low-level expression of CD70, CD95, and CD124. Investigation of the effect of co-crosslinking of various cell surface molecules on both CD20- and BCR-mediated apoptosis in P32/ISH cells (Figures 6 and 7) essentially showed effects on the molecules, CD48, CD55, CD59, CD24, and CD38, similar to those in BALM-24 cells. However, the incidence of the effects was significantly different on the other molecules. For example, enhancement of CD20-mediated apoptosis by co-crosslinking of the molecules, CD19, CD81, CD45, CD70, CD80, CD10, CD22, and CD72, was less significant than observed in BALM-24 cells. Inhibition of CD20-mediated apoptosis by co-crosslinking of the molecules, CD32, CD40, and IL-4 receptor, was also less significant than observed in BALM-24 cells.

Effect of co-crosslinking of CD20 and other cell surface molecules on caspase-3 activity

Next, we investigated whether the caspase cascade is involved in the alteration of CD20-induced apoptosis mediated by co-crosslinking of other molecules. Flow-cytometric analysis with

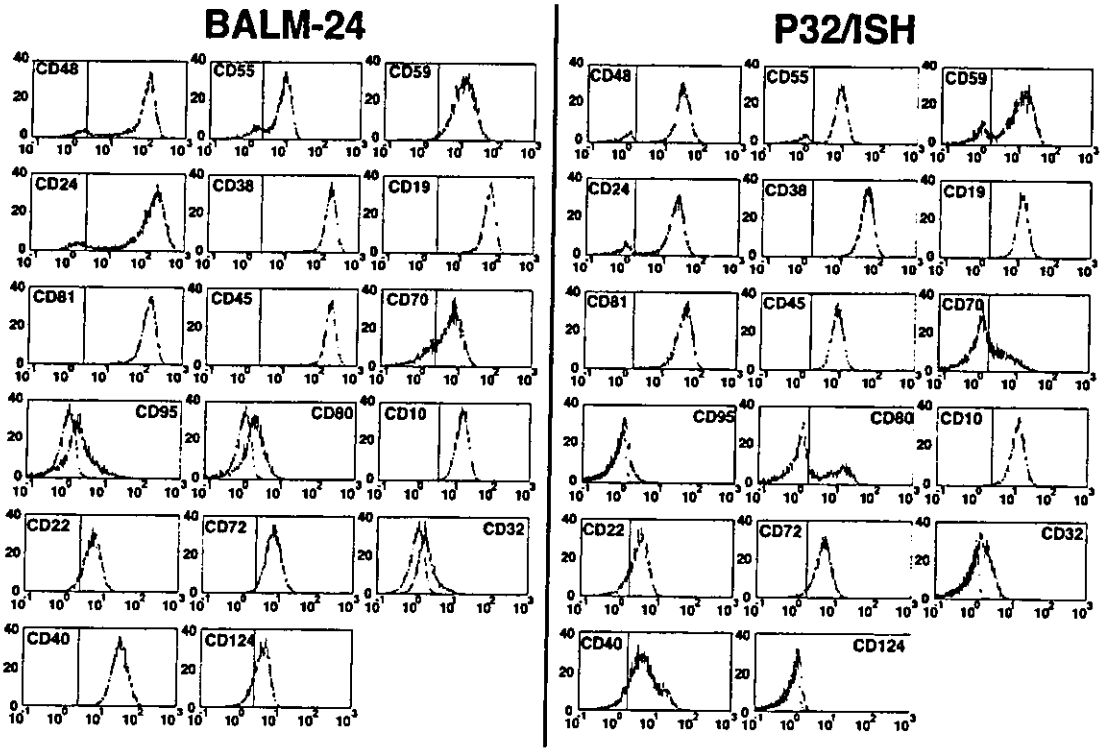

Figure 5 Expression of cell surface antigens on BALM-24 and P32/ISH. BALM-24 cells (left) were stained with FITC-labeled specific mAbs against B-cell differentiation antigens as indicated and analyzed by flow cytometry. The histograms obtained have been displayed as in Figure 1. In the case of the antigens expressed at low levels CD95, CD80, and CD32, the histograms obtained were superimposed on these of the negative controls (cells stained with isotype-matched control mouse immunoglobulin, broken light lines) and displayed. P32/ISH cells (right) were examined in a similar manner. *X*-axis, fluorescence intensity; *Y*-axis, relative cell number.

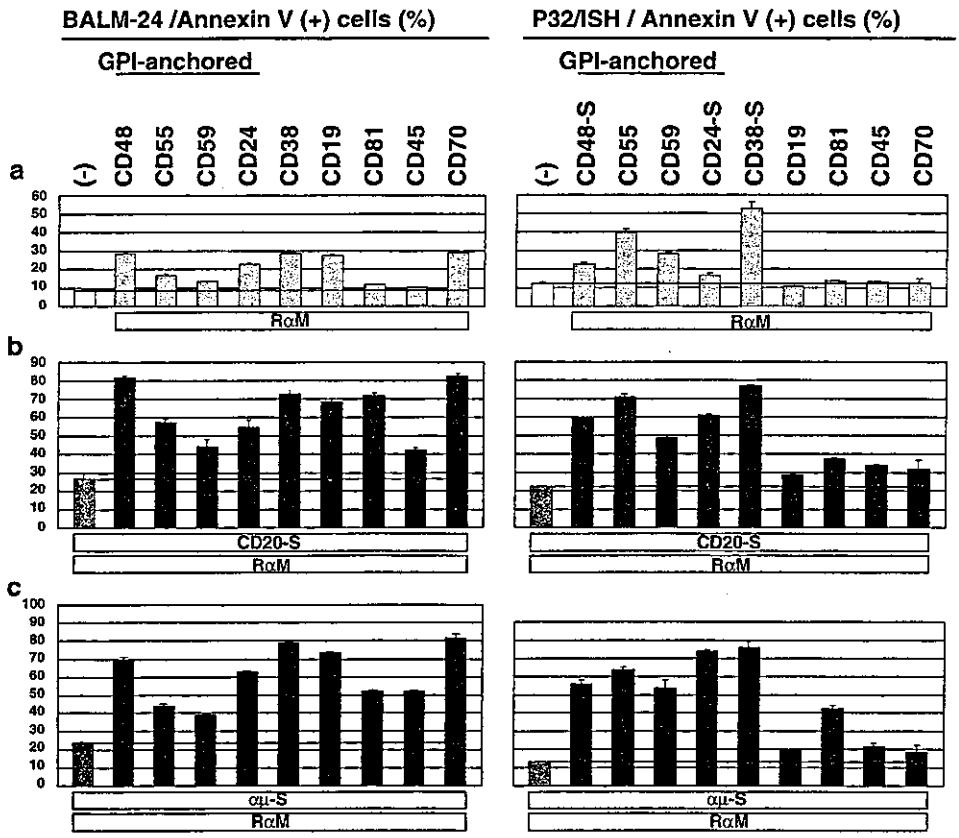

Figure 6 Effect of simultaneous crosslinking of other cell surface antigens on CD20- and B-cell-antigen-receptor (BCR)-mediated apoptosis in BALM-24 and P32/ISH cells. (a) BALM-24 (left) and P32/ISH cells (right) were exposed to monoclonal antibodies (mAbs) against the B-cell differentiation antigens indicated in the presence of secondary rabbit anti-mouse Ig Ab (RαM, 5 μg/ml) for 24 h. A concentration of 5 μg/ml of each mAb was generally used as the full dose, but since crosslinking of CD48, CD24, or CD38 alone induces significant apoptosis in P32/ISH cells, a suboptimal dose (-S, 1 μg/ml each) of mAb was used for CD48, CD24, and CD38 to observe clear synergism with the crosslinking of CD20 and BCR. Apoptotic cells were detected by staining with FITC-conjugated annexin-V as in Figure 2a. (b) Cells were treated as in (a) in the presence of a suboptimal dose of anti-CD20 mAb (CD20-S, 0.5 μg/ml) and examined in a similar manner. (c) Cells were treated as in (a) in the presence of a suboptimal dose of anti-μ mAb (αμ-S, 0.1 μg/ml) and examined in a similar manner.

PhiPhiLux™ G1D2 indicated that co-crosslinking of other molecules affected the numbers of cells in which caspase-3 was activated after crosslinking of CD20 (Figure 8a). As shown in Figure 8a, co-crosslinking of CD32 reduced the number of CD20-mediated caspase-3-activated cells, whereas co-crosslinking of CD80 increased them. Assessment by colorimetric assay with DEVD-*p*NA as the substrate revealed that co-crosslinking of CD32 also significantly reduced the caspase-3 activation induced by CD20 crosslinking (Figure 8b), whereas co-crosslinking of CD80 markedly enhanced caspase-3 activation (Figure 8b). The data indicated that simultaneous crosslinking of other molecules affects activation of caspase cascade induced by CD20 crosslinking.

Effect of co-crosslinking of CD20 and other cell surface molecules on CD20-clustering

The mechanism of enhanced apoptosis caused by co-crosslinking of CD20 and other cell surface molecules is unclear. One possibility is that the costimulation protocol we used in this study simply enhances the extent of CD20 clustering itself, thereby enhancing the apoptotic signal that emerges from CD20 clustering. To test this hypothesis, we used confocal microscopy to examine the extent of CD20 clustering after each treatment. When BALM-24 cells were incubated with Alexa Fluor® 488-conjugated anti-CD20 mAb in the presence of non-labeled secondary rabbit anti-mouse Ab for 30 min at 37°C, CD20 was found to be concentrated in distinct patches within the membrane (Figure 9). When either anti-CD80 or anti-CD32 mAb was added simultaneously, the extent of CD20 clustering on the cell surface did not change significantly. Thus, the results indicate that the alteration of CD20-induced apoptosis mediated by co-crosslinking of other molecules is not merely because of enhanced clustering of CD20 itself.

Effect of independent crosslinking of other cell surface molecules on CD20-mediated apoptosis

We employed the biotin–avidin system to further investigate whether crosslinking between CD20 and other cell surface molecules is necessary for the synergistic or inhibitory effect on induction of apoptosis. As shown in Figure 10, in the presence of avidin (10 μg/ml) a suboptimal dose of biotinylated anti-CD20 mAb (5 μg/ml) induced a low level of apoptosis in BALM-24 cells. When added simultaneously, mAbs against CD19, CD70, and CD80, but not CD45, slightly, but clearly, enhanced the apoptosis induced in BALM-24 cells by a combination of biotinylated anti-CD20 mAb and avidin

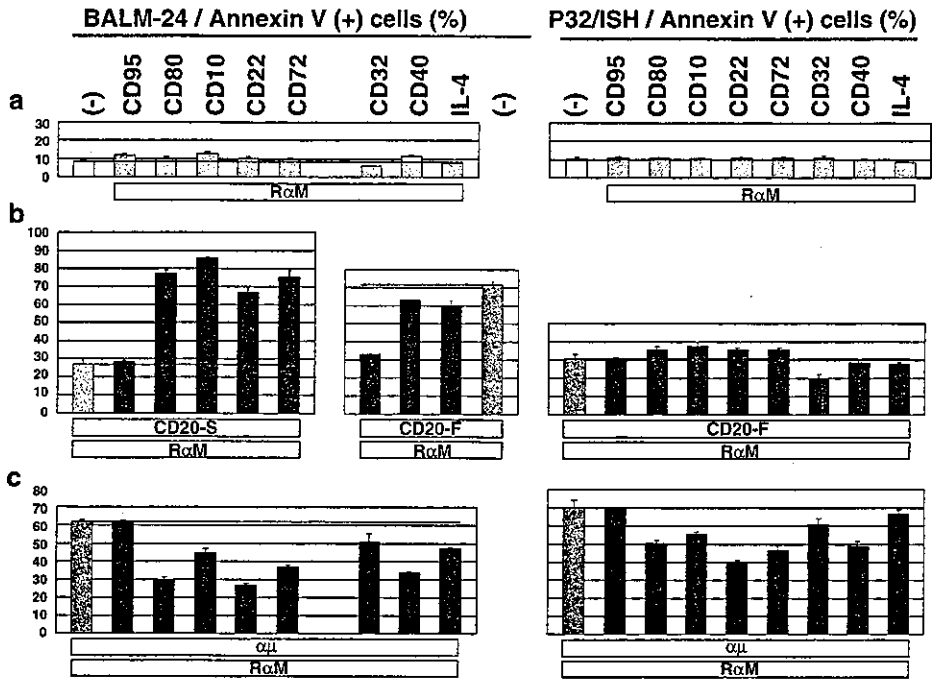

Figure 7 Effect of simultaneous crosslinking of other cell surface antigens on CD20- and B-cell-antigen-receptor-mediated apoptosis in BALM-24 and P32/ISH cells. (a) BALM-24 (left) and P32/ISH cells (right) were exposed to the monoclonal antibodies (mAbs) against B-cell differentiation antigens indicated (5 μg/ml each) or IL-4 (100 ng/ml) in the presence of secondary rabbit anti-mouse Ig Ab (RαM, 5 μg/ml) for 24 h. Apoptotic cells were detected by staining with FITC-conjugated annexin-V as in Figure 2a. (b) Cells were treated as in (a) in the presence of either a suboptimal (-S, 0.5 μg/ml) or full dose (-F, 5 μg/ml) of anti-CD20 mAb (αCD20) and examined in a similar manner. (c) Cells were treated as in (a) in the presence of anti-μ mAb (αμ 5 μg/ml) and examined in a similar manner.

(Figure 10). It should be noted that anti-CD70 induced a low incidence of apoptosis by itself without further ligation by secondary anti-mouse Ab, however, no induction of apoptosis was observed by either CD19 or CD80 alone (Figure 10). By contrast, simultaneous addition of anti-CD32 mAb inhibited the apoptosis induced in BALM-24 cells by the combination of biotinylated anti-CD20 mAb and avidin (Figure 10).

Based on these results, it was concluded that independent crosslinking of each molecule can induce a synergistic and inhibitory effect on the CD20-induced apoptosis. However, the modulatory effect of other cell surface molecules on CD20-mediated apoptosis observed in this experiment was not as significant as that observed in Figures 6 and 7, and independent crosslinking of CD45 had no effect on CD20-mediated apoptosis in this system. Therefore, CD20 and other molecules may need to be clustered together for some part of the modulatory action. Alternatively, some cell surface molecules, such as CD45, may need to be strongly crosslinked by the secondary reagent to exert full regulatory activity on CD20-mediated apoptosis.

DISCUSSION

The caspases, evolutionarily conserved cysteine proteases, have been classified into three distinct groups based on their individual substrate specificities.[26] Group I caspases, caspase-1, -4, and -5, prefer the tetrapeptide sequence WEHD, which occurs in cytokines IL-1 β and IL-18, and thus it participates in the cleavage-mediated activation of these cytokines. The group II caspases, caspase-2, -3, and -7, have optimal peptide recognition of motif DEXD and are thought to be effector proteases that destroy essential homeostatic pathways during the apoptotic process. By contrast, the members of group III, caspase-6, -8, and -9, prefer the peptide sequence recognition motif (L/V)EXD, which resembles the motif at the activation sites of effector caspase proenzymes.

In fact, caspases themselves have been shown to form a regulatory cascade. Apoptotic stimuli mediated by cell surface molecules induce activation of group III upstream caspases, which subsequently directly cleave and activate group II downstream caspases.[27] The downstream caspases go on to cleave various cellular substrates, such as PARP, fodrin, lamin, and ICAD, all of which are responsible for apoptosis.[28] Recently, however, the presence of an alternative mechanism for activation of downstream caspases by upstream caspases has been discovered. Several studies have indicated that activated caspase-8 cleaves Bid, a death agonist member of the Bcl-2/Bcl-x_L family, which in turn induces cytochrome *c* release from mitochondria.[29,30] In response to cytochrome *c*, caspase-9 binds to Apaf-1, the human homologue of *C. elegans* CED-4, becomes activated,[31,32] and then cleaves and activates procaspase-3. A recent study by Besnault *et al*[33] demonstrated involvement of the caspase-8-initiated mitochondria-dependent caspase-3 activation pathway in the process of BCR-mediated apoptosis.

Although the precise mechanism of CD20 induction of apoptosis in BL cells is unknown, caspase-3 has been reported to play a crucial role in the process as an effector.[15,16,24] Our data, however, indicate that activation of multiple caspases is also involved in CD20-induced apoptosis in BL cells. As shown in this study, the peptide inhibitor of caspase-3 reduced CD20-induced apoptosis, but its effect was much weaker than that of z-VAD-fmk, a peptide inhibitor of a broad range of caspases, suggesting involvement of other caspases than caspase-3 as

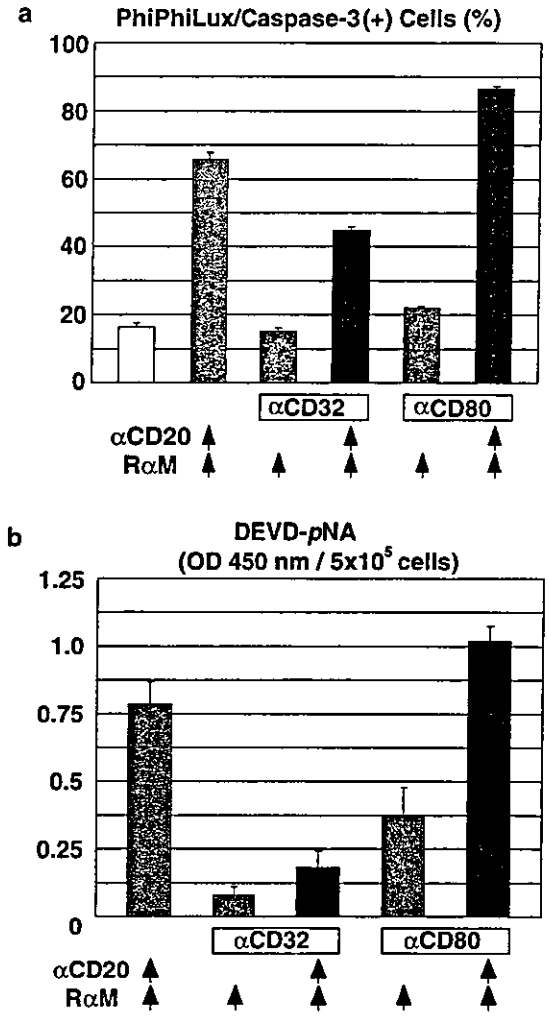

Figure 8 Effect of simultaneous crosslinking of CD32 and CD80 on CD20- and B-cell-antigen-receptor-mediated apoptosis in BALM-24 cells. (a) BALM-24 cells were exposed to a combination of anti-CD20 monoclonal antibody (mAb) (αCD20, 5 μg/ml), anti-CD32 mAb (αCD32, 5 μg/ml), and anti-CD80 mAb (αCD80, 5 μg/ml), in the presence of secondary RαM Ab (5 μg/ml) for 24 h and subsequent caspase-3 activity was measured by flow-cytometry with PhiPhiLux™ GiD2. (b) After the same treatment as in (a), subsequent caspase-3 activity was measured by colorimetric assay using specific peptide substrate DEVD-*p*NA.

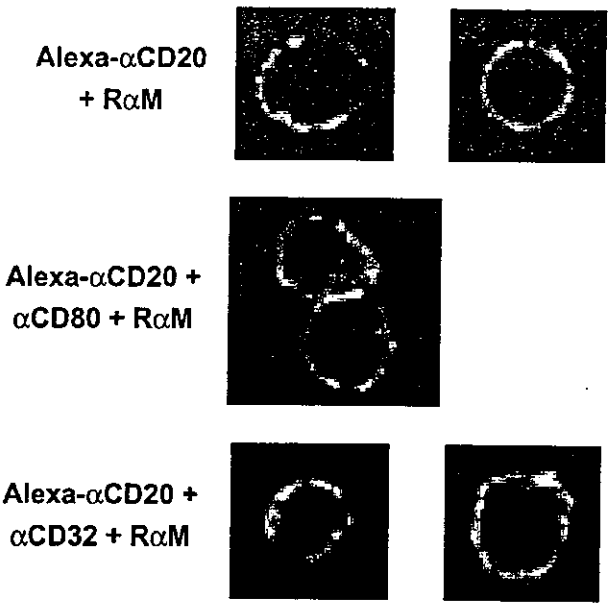

Figure 9 CD20 clustering on BALM-24 cells after treatment with anti-CD20 mAb. To observe the extent of CD20 clustering on the cell surface, cells were incubated for 30 min at 37°C with a combination of Alexa Fluor® 488-conjugated anti-CD20 (αCD20) mAb and non-labeled anti-CD80 (αCD80) or anti-CD32 (αCD32) mAb in the presence of non-labeled secondary rabbit anti-mouse (RαM) polyclonal Ab. After intensive washing with ice-cold PBS and fixation with 3% paraformaldehyde in PBS, cells were examined by confocal microscopy. Typical results from each treatment are shown.

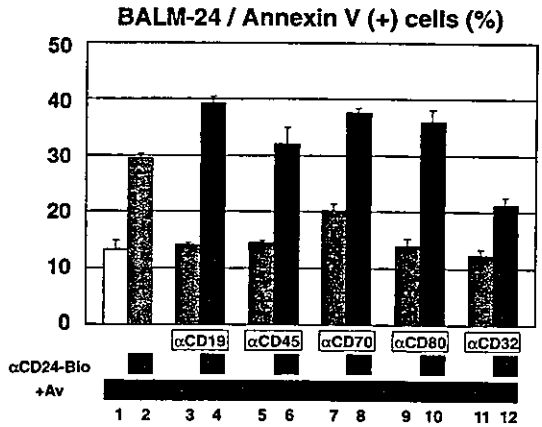

Figure 10 Effect of independent crosslinking of other cell surface antigens on CD20-mediated apoptosis in BALM-24 cells. CD20 molecules expressed on BALM-24 cells were crosslinked with a combination of 5.0 μg/ml of biotin-conjugated anti-CD20 monoclonal antibody (mAb) and 10 μg/ml of avidin, as indicated. A 5.0 μg/ml dose of mAbs against CD19, CD45, CD70, CD80, and CD32 were added simultaneously as indicated. After 24-h incubation, the incidence of apoptotic cells was examined as in Figure 3.

effectors of the apoptotic process. Immunoblot analysis has consistently indicated activation of multiple caspases, including caspase-2, -7, -8, and -9. The current model of the regulatory cascade of caspases suggested that caspase-2 and -7, both of which are classified as group II caspases, act as effector caspases the same as caspase-3. By contrast, caspase-8 and -9 are thought to participate in activating these downstream caspases in the process of CD20-mediated apoptosis. Indeed, as we have shown in this study, the evidence that the peptide inhibitor of caspase-8 and -9 inhibited the activation of caspase-3 induced by CD20 crosslinking supports this notion. This evidence together with the evidence of cleavage of Bid indicate that mitochondria-dependent activation of caspase-3 is involved in CD20-induced apoptosis. However, the effect of caspase-9 inhibitor in reducing CD20-mediated caspase-3 activation is less than that of caspase-8 inhibitor, and thus not only the mitochondria-dependent pathway but also other mechanisms, such as direct cleavage of caspase-3 by -8, may participate in the CD20-mediated activation of caspase-3. All of the above findings suggest involvement of multiple caspase cascades in the process of CD20-induced apoptosis.

In the process of B-cell differentiation, signals mediated by BCR primarily determine whether B cells survive or not, but other stimuli mediated by surface-expressing molecules coop-

erate in regulating this process.[2–6] Although the functional role of CD20 in a physiological context remains unclear, it can be argued that CD20 is a signal-transduction-related molecule. Since, as shown in this study, CD20-mediated stimuli significantly augment BCR-mediated apoptosis induction in BL cells, CD20 may participate in clonal selection of B cells as an enhancer of BCR-mediated negative signals.

Our findings clearly indicate that other cell surface molecules in addition to CD20 are involved in survival and death signaling in B cells. Based on their behavior in terms of BCR- and CD20-mediated apoptosis, cell surface molecules can be classified into several groups. First, GPI-anchored proteins, CD24, CD48, CD55, and CD59, which induce apoptosis in BL cells upon crosslinking by themselves,[22] synergistically affect both BCR- and CD20-mediated apoptosis. Other molecules, CD38,[34] CD19, and CD70, exhibit behavior similar to that of GPI-anchored proteins. Second, CD81 and CD45 do not induce apoptosis by themselves, but they clearly enhanced the apoptosis-inducing effect of both CD20 and BCR upon simultaneous crosslinking.

By contrast, the molecules known to mediate inhibitory signals for BCR, such as CD32, CD40, and CD124, down-regulate the apoptosis induction mediated by both BCR and CD20. Since CD20 enhances BCR-mediated apoptotic signals, it is not surprising that these molecules also mediate inhibitory signals for CD20. CD72, however, which is known as an another inhibitory coreceptor for BCR, inhibits BCR-mediated apoptosis but enhances CD20-mediated apoptosis. The behavior of other molecules, CD10, CD22, and CD80, is similar to that of CD72. How these molecules affect BCR- and CD20-mediated apoptosis differently still remains unclear, our findings indicate the complexity of the crosstalk between regulatory signals for cell survival and death induced by cell surface molecules. It should also be noted that the modulatory effects of co-crosslinking of other molecules on CD20-induced apoptosis vary significantly between cell lines as we presented in this study.

It is worth noting that CD95, a Fas antigen, neither induced apoptosis by itself nor enhanced CD20-mediated apoptosis in BALM-24 cells. Since CD95 has been reported to play an important role in activation-induced cell death and elimination of autoreactive B cells,[35] our data may mean that this molecule has a role in B cells distinct from that mediated by BCR and CD20 in B cells.

Although the mechanism of enhancement of CD20-induced apoptosis mediated by co-crosslinking of other molecules is unknown, one possibility is that the co-crosslinking protocol used in this study simply enhances the extent of CD20 clustering itself, thereby enhancing the apoptotic signal that emerges from CD20 clustering. However, since the results of confocal microscopy in this study indicate that CD20 clustering is unaffected by co-crosslinking with either CD80 or CD32, the modulatory effect of other molecules is not merely because of alteration of the efficiency of CD20 clustering. Moreover, as shown in this study, independent crosslinking of CD19, CD80, and CD32 has a synergistic and inhibitory effect on CD20-mediated apoptosis, respectively. Thus, some part of the above-described regulatory action on apoptosis is most likely achieved by crosstalk between the signals mediated by these molecules and by CD20. Further studies to elucidate the precise mechanism of the modulatory effect of other molecules on CD20-mediated apoptosis are now under way.

In this study, we also found that enhancement and inhibition of CD20-induced apoptosis by other costimulatory signals are accompanied by alterations of caspase activity. For example, when CD20-induced apoptosis is enhanced by co-crosslinking with CD80, caspase-3 activity is enhanced. By contrast, CD32-mediated inhibition of CD20-induced apoptosis is accompanied by a reduction of caspase-3 activation. How co-stimulation of CD20 and other molecules induces alterations of caspase activation is unknown, but our findings indicate that regulation of apoptosis induction mediated by crosstalk between co-stimulatory signals is achieved by modification of caspase activation.

In conclusion, the findings described above suggest that CD20-mediated apoptosis is closely correlated with that mediated by BCR, whereas these two apoptosis inducing signals are differently regulated by other co-stimulatory signals in B cells, at least in part. Although additional study is clearly necessary, investigation of CD20-mediated apoptosis and its regulation by other cell surface molecules should provide a new approach to understanding the regulation of clonal selection of B cells and to the establishment of a new therapeutic approach for BL patients. The finding of marked enhancement of apoptosis induction by simultaneous crosslinking of CD20 and other molecules, in particular, seems likely to provide a more effective strategy for Ab-mediated apoptosis induction therapy of B-cell malignancies.

Acknowledgements

This work was supported in part by a Grant for Pediatric Research (12C-01) from the Ministry of Health and Welfare of Japan and a Grant by Children's Cancer Association of Japan. This work was also supported by the Program for Promotion of Fundamental Studies in Health Sciences of the Organization for Drug ADR Relief, R & D Promotion and Product Review of Japan and by a grant from the Japan Health Sciences Foundation for Research on Health Sciences Focusing on Drug Innovation. Additional support was provided by the Program of the Research and Development Promotion Division, Science and Technology Promotion Bureau, STA for Organized Research Combination System. We thank M Sone and S Yamauchi for their excellent secretarial works.

References

1 Uckun FM. Regulation of human B-cell ontogeny. *Blood* 1990; **76**: 1908–1923.
2 Rajewsky K. Clonal selection and learning in the antibody system. *Nature* 1996; **381**: 751–758.
3 Goodnow CC. Balancing immunity and tolerance: deleting and tuning lymphocyte repertoires. *Proc Natl Acad Sci USA* 1996; **93**: 2264–2271.
4 Buhl AM, Cambier JC. Co-receptor and accessory regulation of B-cell antigen receptor signal transduction. *Immunol Rev* 1997; **160**: 127–138.
5 O'Rourke L, Tooze R, Fearon DT. Co-receptors of B lymphocytes. *Curr Opin Immunol* 1997; **9**: 324–329.
6 Tsubata T. Co-receptors on B lymphocytes. *Curr Opin Immunol* 1999; **11**: 249–255.
7 Tedder TF, Engel P. CD20: a regulator of cell-cycle progression of B lymphocytes. *Immunol Today* 1994; **15**: 450–454.
8 Deans JP, Schieven GL, Shu GL, Valentine MA, Gilliland LA, Aruffo A *et al*. Association of tyrosine and serine kinases with the B cell surface antigen CD20. Induction via CD20 of tyrosine phosphorylation and activation of phospholipase C-gamma 1 and PLC phospholipase C-gamma 2. *J Immunol* 1993; **151**: 4494–4504.
9 Deans JP, Kalt L, Ledbetter JA, Schieven GL, Bolen JB, Johnson P. Association of 75/80-kDa phosphoproteins and the tyrosine kinases Lyn, Fyn, and Lck with the B cell molecule CD20.

Evidence against involvement of the cytoplasmic regions of CD20. *J Biol Chem* 1995; **270**: 22632–22638.
10 Mathas S, Rickers A, Bommert K, Dorken B, Mapara MY. Anti-CD20- and B-cell receptor-mediated apoptosis: evidence for shared intracellular signaling pathways. *Cancer Res* 2000; **60**: 7170–7176.
11 Bubien JK, Zhou LJ, Bell PD, Frizzell RA, Tedder TF. Transfection of the CD20 cell surface molecule into ectopic cell types generates a Ca^{2+} conductance found constitutively in B lymphocytes. *J Cell Biol* 1993; **121**: 1121–1132.
12 Shan D, Ledbetter JA, Press OW. Apoptosis of malignant human B cells by ligation of CD20 with monoclonal antibodies. *Blood* 1998; **91**: 1644–1652.
13 McLaughlin P, Grillo-Lopez AJ, Link BK, Levy R, Czuczman MS, Williams ME *et al*. Rituximab chimeric anti-CD20 monoclonal antibody therapy for relapsed indolent lymphoma: half of patients respond to a four-dose treatment program. *J Clin Oncol* 1998; **16**: 2825–2833.
14 Reff ME, Carner K, Chambers KS, Chinn PC, Leonard JE, Raab R *et al*. Depletion of B cells *in vivo* by a chimeric mouse human monoclonal antibody to CD20. *Blood* 1994; **83**: 435–445.
15 Hofmeister JK, Cooney D, Coggeshall KM. Clustered CD20 induced apoptosis: src-family kinase, the proximal regulator of tyrosine phosphorylation, calcium influx, and caspase 3-dependent apoptosis. *Blood Cells Mol Dis* 2000; **26**: 133–143.
16 Shan D, Ledbetter JA, Press OW. Signaling events involved in anti-CD20-induced apoptosis of malignant human B cells. *Cancer Immunol Immunother* 2000; **48**: 673–683.
17 Chaouchi N, Vazquez A, Galanaud P, Leprince C. B cell antigen receptor-mediated apoptosis. Importance of accessory molecules CD19 and CD22, and of surface IgM crosslinking. *J Immunol* 1995; **154**: 3096–3104.
18 Matsuo Y, Sugimoto A, Harashima A, Nishizaki C, Ishimaru F, Kondo E *et al*. Establishment and characterization of a novel ALL-L3 cell line (BALM-18): induction of apoptosis by anti-IgM and inhibition of apoptosis by bone marrow stroma cells. *Leukemia Res* 1999; **23**: 559–568.
19 Diebold J, Jaffe ES, Raphael M, Warnke RA. Burkitt lymphoma. In: Jaffe ES, Harris NL, Stein H, Vardiman JW (eds). *World Health Organization Classification. Tumours of Haematopoietic and Lymphoid Tissues*. Lyon: IARC Press, 2001; pp. 181–184.
20 Fujimoto J, Ishimoto K, Kiyokawa N, Tanaka S, Ishii E, Hata J. Immunocytological and immunochemical analysis on the common acute lymphoblastic leukemia antigen (CALLA): evidence that CALLA on ALL cells and granulocytes are structurally related. *Hybridoma* 1988; **7**: 227–236.
21 Kokai Y, Ishii Y, Kikuchi K. Characterization of two distinct antigens expressed on either resting or activated human B cells as defined by monoclonal antibodies. *Clin Exp Immunol* 1986; **64**: 382–391.
22 Suzuki T, Kiyokawa N, Taguchi T, Sekino T, Katagiri YU, Fujimoto J. CD24 induces apoptosis in human B cells via the glycolipid-enriched membrane domains/rafts-mediated signaling system. *J Immunol* 2001; **166**: 5567–5577.
23 Suzuki J, Fujita J, Taniguchi S, Sugimoto K, Mori KJ. Characterization of murine hemopoietic-supportive (MS-1 and MS-5) and non-supportive (MS-K) cell lines. *Leukemia* 1992; **6**: 452–458.
24 Henkart PA. ICE family proteases: mediators of all apoptotic cell death? *Immunity* 1996; **4**: 195–201.
25 Chinnaiyan AM, Dixit VM. The cell-death machine. *Curr Biol* 1996; **6**: 555–562.
26 Thornberry NA, Rano TA, Peterson EP, Rasper DM, Timkey T, Garcia-Calvo M *et al*. A combinatorial approach defines specificities of members of the caspase family and granzyme B. Functional relationships established for key mediators of apoptosis. *J Biol Chem* 1997; **272**: 17907–17911.
27 Yang X, Chang HY, Baltimore D. Autoproteolytic activation of pro-caspases by oligomerization. *Mol Cell* 1998; **1**: 319–325.
28 Nagata S. Apoptosis by death factor. *Cell* 1997; **88**: 355–365.
29 Li H, Zhu H, Xu CJ, Yuan J. Cleavage of BID by caspase 8 mediates the mitochondrial damage in the Fas pathway of apoptosis. *Cell* 1998; **94**: 491–501.
30 Luo X, Budihardjo I, Zou H, Slaughter C, Wang X. Bid, a Bcl2 interacting protein, mediates cytochrome *c* release from mitochondria in response to activation of cell surface death receptors. *Cell* 1998; **94**: 481–490.
31 Cecconi F, Alvarez-Bolado G, Meyer BI, Roth KA, Gruss P. Apaf1 (CED-4 homolog) regulates programmed cell death in mammalian development. *Cell* 1998; **94**: 727–737.
32 Li P, Nijhawan D, Budihardjo I, Srinivasula SM, Ahmad M, Alnemri ES *et al*. Cytochrome *c* and dATP-dependent formation of Apaf-1/caspase-9 complex initiates an apoptotic protease cascade. *Cell* 1997; **91**: 479–489.
33 Besnault L, Schrantz N, Auffredou MT, Leca G, Bourgeade MF, Vazquez A. B cell receptor crosslinking triggers a caspase-8-dependent apoptotic pathway that is independent of the death effector domain of Fas-associated death domain protein. *J Immunol* 2001; **167**: 733–740.
34 Kumagai M, Coustan-Smith E, Murray DJ, Silvennoinen O, Murti KG, Evans WE *et al*. Ligation of CD38 suppresses human B lymphopoiesis. *J Exp Med* 1995; **181**: 1101–1110.
35 Fukuyama H, Adachi M, Suematsu S, Miwa K, Suda T, Yoshida N, Nagata S. Transgenic expression of Fas in T cells blocks lymphoproliferation but not autoimmune disease in MRL-lpr mice. *J Immunol* 1998; **160**: 3805–3811.

Available online at www.sciencedirect.com
SCIENCE DIRECT®
PERGAMON
Molecular Immunology 39 (2003) 871–878
Molecular Immunology
www.elsevier.com/locate/molimm

Catalytic RAG1 mutants obstruct V(D)J recombination in vitro and in vivo

Tadashi Furusawa [a], Misa Hosoe [a], Katsuhiro Ohkoshi [a], Seiya Takahashi [b], Nobutaka Kiyokawa [c], Jun-ichiro Fujimoto [c], Hiroshi Amemiya [c], Seiichi Suzuki [c,1], Tomoyuki Tokunaga [a,*]

[a] *Development and Differentiation Laboratory, Developmental Biology Department, Insect and Animal Sciences Division, National Institute of Agrobiological Sciences, Ikenodai 2, Kukisaki, Inashiki, Ibaraki 305-8602, Japan*
[b] *Reproductive Cell biology Laboratory, Department of Animal Breeding and Reproduction, National Institute of Livestock and Grassland Science, Ikenodai 2, Kukisaki, Inashiki, Ibaraki 305-0901, Japan*
[c] *National Research Institute for Child Health and Development, Taishido 3-35-31, Setagaya-ku, Tokyo 154-8567, Japan*

Received 4 December 2002; received in revised form 2 January 2003; accepted 17 January 2003

Abstract

To generate severe combined immunodeficient (SCID) livestocks for xenotransplantation, we have attempted to generate a SCID phenotype without gene knockout. Based on the reported mouse RAG1 mutants, we constructed the corresponding rabbit RAG1 mutants by mutagenesis of three residues within the catalytic domain: D602A, D710A, and E964A. As expected, these mutants each exhibited no catalytic activity on artificial substrates and inhibited recombination by the wild type RAG1. Moreover, replacement of the N-terminus of RAG1 with enhanced green fluorescent protein (EGFP) greatly increased protein stability, and the triple mutant RAG1 showed a twofold increase in its ability to inhibit wild type activity in vitro. We generated mice transgenic for the latter mutant to assess its effect on V(D)J recombination in vivo. Serum IgM levels in four out of seven transgenic mice were reduced to approximately 30–50% of control levels in four out of seven transgenic mice. Our results suggest that immunodeficient animals for regenerative medicine could be generated without gene knockout.

Keywords: Xenotransplantation; SCID; RAG1 mutants

1. Introduction

Xenotransplantation is a potential solution to the chronic shortage of human donor organs. Although clinical obstacles to this approach are more formidable than with human-to-human transplantation, progress has been made to prevent the hyperacute rejection (HAR) of donor tissues by the recipient's immune system. In addition to the development of immunosuppressive drugs (Lei et al., 2000), organs from transgenic animals that express human complement regulatory proteins, including decay accelerating factor (DAF), membrane co-factor protein (MCP), and CD59, are expected to be of therapeutic use (Rosengard et al., 1995). However, even if HAR were completely suppressed, xenogeneic organs would still produce large amounts of foreign proteins, especially in the case of liver transplantation, that could result in the activation of the patient's immune system. To address this problem, we aim to create a hybrid liver consisting of human hepatocytes within a framework of blood vessels and bile ducts from the pig. A severe combined immune deficient (SCID) pig that accepts human cells without rejection would be required to grow such organs. Our goal is to use an in utero manipulation technique (IUM) to replace porcine hepatocytes with their human counterparts in a transgenic SCID pig fetus expressing human DAF (Enosawa et al., 2001a,b; Fujino et al., 2001). Although several SCID lineages have been generated by gene disruption in murine embryonic stem (ES) cells (Gao et al., 1998a,b; Gu et al., 1997; Mombaerts et al., 1992; Shinkai et al., 1992; Zhu et al., 1996), the ES cell approach is not feasible in livestock such as pigs and rabbits. Somatic cell nuclear transplantation has been successful in pigs (Onishi et al., 2000; Polejaeva et al., 2000), and piglets with disruption of one allele of the α1,3 galactosyltransferase locus have been produced (Dai et al., 2002; Lai et al., 2002). Nevertheless, homologous recombination in somatic cells is quite inefficient and the technique has

* Corresponding author. Tel.: +81-29-838-7384; fax: +81-29-838-73823.
E-mail address: tom@affrc.go.jp (T. Tokunaga)
[1] Deceased on 14 August 2002.

0161-5890/03/$ – see front matter
doi:10.1016/S0161-5890(03)00008-7

not been optimized. As a preliminary step towards our goal of creating SCID livestock, we have used transgenic techniques to create small animals with the SCID phenotype.

In vertebrates, V(D)J recombination plays a critical role in the generation of antigen receptor diversity in B and T cells (Tonegawa, 1983). V(D)J recombination is initiated by the association of two proteins, recombination activating gene (RAG) 1 and RAG 2 (Oettinger, 1992; Schatz et al., 1989), at the recombination signal sequences (RSS) (Max et al., 1979; Sakano et al., 1979). This leads to the nicking of one DNA strand between the RSS and the coding sequence. Although both RAG1 and RAG2 are essential for recombination (McBlane et al., 1995), only RAG1 has a direct role in DNA cleavage (Kim et al., 1999; Landree et al., 1999). To date, there have been many efforts to identify catalytic mutants of RAG1 (Aidinis et al., 2000; Kim et al., 1999; Landree et al., 1999; Li et al., 2001; Lin et al., 1999; McMahan et al., 1997; Noordzij et al., 2000; Sadofsky et al., 1993; Schwarz et al., 1996; Steen et al., 1999; Villa et al., 1998, 2001; Yarnell Schultz et al., 2001). We have focused on catalytic mutants that retain normal RSS binding to develop derivatives with dominant negative activity against the wild type protein (Kim et al., 1999; Landree et al., 1999). Seven point-mutant RAG1 proteins were generated and their activities were assessed in vitro using an artificial substrate plasmid that enabled recombination frequency to be reported as luciferase activity.

In this report, we describe catalytic RAG1 mutants that bind normally to DNA, but that inhibit the activity of wild type RAG1. Moreover, the replacement of the N-terminus of RAG1 with the enhanced green fluorescent protein (EGFP) increased the inhibition activity in vitro, and transgenic mice carrying this mutant gene showed low serum IgM levels. These data suggest that immunodeficient animals could be generated without gene disruption and that this strategy is applicable to almost any vertebrate species.

2. Materials and methods

2.1. Cloning of rabbit RAG1 and RAG2 gene

Because the coding regions of both rabbit *RAG* genes were contained in signal exons, they were amplified from genomic DNA by the polymerase chain reaction (PCR). Primer sequences were based on the reported nucleotide sequences (RAG1, M77666; RAG2, M77667) with *Eco*RI or *Not*I sites added to their 5′ ends. The *RAG1* gene was amplified in two segments with the following primers: RAG1S1, 5′-AAGGATCCATCATGGCTGTGTCTTGC-3′; RAG1AS1, 5′-AAGCGGCCGCCTTGACTTGTAACTTC-AGCTCC-3′; RAG1S2, 5′-AAGGATCCCGTCAACATCT-CCTATCG-3′; RAG1AS2, 5′-AAGCGGCCGCATAAGTG-GTTGAACCCTCC-3′. To reconstitute the full-length *RAG1* gene, the subcloned fragments were joined at a unique *Sac*I site in each fragment. The *RAG2* gene was amplified with the following primers: RAG2S1, 5′-AA-GAATTCGAAAACATGTCGCTGCAGATG-3′; RAG2AS1 5′-AAGCGGCCGCAAAATTAGTCAAACAACCGTC-3′.

2.2. Mutagenesis and expression vectors

Three amino acid mutations D602A, D710A, and E964A were introduced into RAG1 by PCR-assisted DNA mutagenesis, and double/triple mutants were also generated. Wild-type and mutant *RAG1* genes were subcloned into the pCDNA3.1(−)/Myc-His expression vector (Invitrogen, Carlsbad, CA, USA), with a myc-His tag sequence fused to the 3′-terminus. To generate truncated RAG1 proteins, core domains (residues 380–1042) were amplified by PCR with the following primers: RAG1S3, 5′-AAGGATCCATGGAA-TCAAGAGATACTTTTGTGCA-3′; RAG1AS3, 5′-TTAA-GCTTAAATTCCATTGAATATTGGC-3′. Amplified fragments derived from both the wild type and point-mutant *RAG1* genes were subcloned into the pCDNA3.1(−)/Myc-His expression vector with the *EGFP* gene from pEGFP-C1 (Invitrogen) inserted in-frame at the *Bam*HI site at the 5′ end of each derivative. The *RAG2* gene was subcloned into the pCDNA3 expression vector (Invtrogen). The fidelity of PCR and recombination was confirmed by DNA sequencing.

2.3. Cell cultures

NIH3T3 and Cos7 cells were cultured in Dulbecco's modified Eagle's medium (GIBCOBRL, Grand Island, NY, USA) supplemented with 10% fetal bovine serum (FBS).

2.4. In vitro recombination assay

The recombination substrate vector, pRSSLuc, carried the puromycin^r (*puro*^{r}) gene and the PGK polyadenylation signal flanked by two synthetic recombination signal sequences, 12-RSS and 23-RSS. Expression of the *puro*^{r} gene was driven by the chicken β-actin (CAG) promoter originated from pCAGGS vector (Miyazaki et al., 1989) placed upstream of the 12-RSS. The firefly luciferase (*Luc*) gene, derived from pGV-B2 vector (Toyo inki, Tokyo, Japan), was placed downstream of the 23-RSS, followed by the rabbit β-globin polyadenylation signal. RAG-mediated joining of the two RSSs removes the puro^r and PGK polyadenylation signal by DNA deletion, and places the *Luc* gene immediately downstream of the CAG promoter (Fig. 2). Plasmids were transiently transfected into NIH3T3 cells using LIPOFECTAMINE Plus Reagent (GIBCO-BRL) following the manufacturer's protocols. Briefly, 0.2 μg of pRSSLuc, 0.1 μg of the RAG2 expression vector, 0.1 μg of the wild type-RAG1 expression vector, 0.1 μg of pRL-TK (*Renilla* luciferase expression vector, Promega, Madison, WI, USA), and 0.1–0.2 μg of the mutant RAG1 expression vector were co-transfected into cells on 24-well plates. The amount of total plasmid DNA was made equivalent by the addition of pcDNA3.1(−)/MycHis/lacZ vector DNA

(Invtrogen) because the *Escherichia coli*, *β-galactosidase* gene was almost equivalent in size to the *RAG1* gene. Cells were harvested after 40–48 h and firefly and *Renilla* luciferase activities were measured using the Dual Luciferase Reporter Assay System (Promega). The firefly luciferase activity was normalized to the *Renilla* luciferase activity.

2.5. Western blot analysis

Cos7 cells were rinsed with PBS and harvested by scraping in cold RIPA buffer (50 mM Tris–HCl, pH 8.0, 150 mM NaCl, 0.5% deoxycholate, 1% NP-40) containing protease inhibitors (Complete EDTA-free, Roche Molecular Biochemicals, Mannheim, Germany). Protein samples (50 μg per lane) were subjected to SDS-polyacrylamide gel electrophoresis (SDS-PAGE). After electrophoresis, proteins were electrophoretically transferred onto PVDF membranes. Proteins on the membranes were probed with anti-myc antibody (Clontech), and bound antibodies were visualized with the ECL Western detection system (Amersham Biosciences, Piscataway, NJ, USA).

2.6. Generation of transgenic mice

GFP fused to the mutant *RAG1* gene was inserted at the *EcoR*I site of the pCAGGS vector. A purified DNA fragment containing the GFP-mutant RAG1 fusion gene, CAG promoter and rabbit β-globin polyadenylation signal, but lacking the vector backbone was dissolved in PBS to 10 ng/μl. Matured female F1 (DBA × C57Bl/6J) mice (Charles River Japan, Kanagawa, Japan) were superovulated by intraperitoneal injection of 5 IU of pregnant mare's serum gonadotrophin (SEROTOROPIN, TEIKOKU HORMONE MSG, Tokyo, Japan) followed 48 h later by 5 IU of human chorionic gonadotrophin (PUBEROGEN, Sankyo, Tokyo, Japan), and then mated with ICR male mice (Charles River Japan). Fertilized eggs were collected from the fallopian tubes 20 h after hCG injection, and were microinjected with ~2 pl of the DNA solution into the male pronucleus. Eggs were cultured in M16 medium (Sigma, St. Louis, MO, USA) for 16–20 h at 37 °C in a 5% CO_2/air, and then transplanted into the fallopian tubes of pseudopregnant ICR mothers.

2.7. Enzyme linked immunosorbent assay (ELISA)

F16 MaxiSorp plates (NUNC, Roskilde, Denmark) were coated with 40 ng/well of rabbit anti-mouse IgM (61-6800, Zymed Labolatories, CA, USA) and incubated with blocking buffer (3% bovine serum albumin containing PBS). Diluted mouse sera were added to the ELISA plate wells, and incubated for 1 h at room temperature. After washing with buffer (0.02% Tween-20 containing PBS), 1:2000 diluted horseradish peroxidase (HRP) conjugated goat anti-mouse IgM (62-6820, Zymed Labolatories) was added. After 1 h incubation and washing, bound antibodies were detected by *o*-phenylenediamine (OPD). Serum IgM concentrations were calculated using purified mouse IgM (02-6800, Zymed Labolatories) as a standard.

3. Results

3.1. Construction of RAG1 mutants

We first created RAG1 catalytic mutants that retained DNA-binding activity and maintained their interaction with protein partners involved in DNA recombination. Landree et al. (1999) and Kim et al. (1999) previously described mutants in the mouse RAG1 protein with intact DNA binding activity, but lacking DNA cleavage activity. Based on these reports, we mutated three residues in the rabbit RAG1 protein: D602A, D710A, and E964A, located in the catalytic domain, and evolutionarily conserved between fish and mammals (Fig. 1A and B). All seven mutants, including double/triple mutants (D602A/D710A, D602A/E964A, D710A/E964A, and D602A/D710A/E964A), and wild-type RAG1 were introduced a myc-His tag at the C-terminus.

3.2. RAG1mutants inhibited recombination by wild type RAG1 in vitro

To measure the catalytic activity of RAG1 protein, we established an in vitro recombination assay system using the pRSSLuc artificial substrate vector, which contains two RSSs (Fig. 2). We confirmed the RAG-dependent DNA recombination of the two RSSs by direct sequencing of PCR products recovered from transfected cells (data not shown). Myc-His tagged RAG1 protein showed similar activity to non-tagged, wild type RAG1 in this assay, indicating that the tag did not affect RAG1 recombination activity. In contrast, D602A, D710A, E964A, and double/triple mutant RAG1 proteins were completely inactive (Fig. 3). Furthermore, co-transfection of equivalent amounts of mutant and wild type *RAG1* genes decreased the recombination frequency of the RSS substrate vector to 50% of the control value.

Myc-His tagged wild type RAG1 protein was barely detectable (Fig. 4A) by Western blot analysis with anti-myc antibody, suggesting that the half-life of RAG1 proteins was quit short in vivo. There are reports that N-terminal truncation of RAG1 protein increases its stability (Silver et al., 1993; McMahan et al., 1997; Steen et al., 1999). To prolong the half-life of RAG1 proteins, we constructed a RAG1 variant comprising N-terminal residues, 1–379, fused to the GFP protein at the N-terminus, allowing easy detection of expression (GFPwtRAG1, see Fig. 1A). We clearly detected the GFPwtRAG1 protein by Western blot analysis (Fig. 4A), and found that it produced twofold greater recombination of the RSS substrate vector than the wild type RAG1 protein (Fig. 4B). In co-transfection experiments, GFPmutRAG1 (GFP fused to the triple mutant RAG1) inhibited the recombination in a dose-dependent manner and exhibited a twofold increase in inhibition activity compared to non-truncated RAG1 mutants (Fig. 4C).

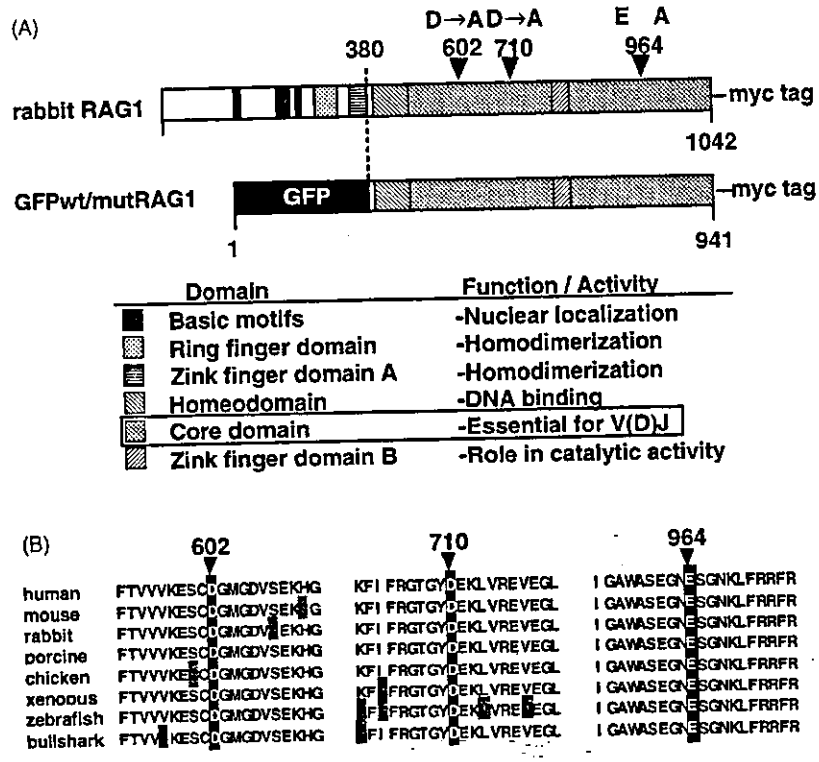

Fig. 1. (A) Schematic diagram of the rabbit RAG1 protein indicating the positions of the three mutations used in this study. GFPwt/mutRAG1 is shown below, and is a derivative whose N-terminal domain (1–379) has been replaced with GFP protein. The various domains and their functions are indicated below the diagram (Villa et al., 2001). (B) Alignment of the catalytic residues at the core domain of rabbit RAG1 with other vertebrates. Highlighted amino acid residues show the position of mutations.

3.3. *Transgenic mice carrying the GFPmutRAG1 gene showed low serum IgM levels*

Next, we generated mice transgenic for the GFPmutRAG1 gene to examine the ability of this mutant RAG1 to inhibit V(D)J recombination in vivo. The CAG promoter was used to confer ubiquitous and strong expression to the mutant RAG1 protein. Although no pups exhibited strong green fluorescence under UV light, seven transgenic mice were identified by PCR analysis of genomic DNA extracted from

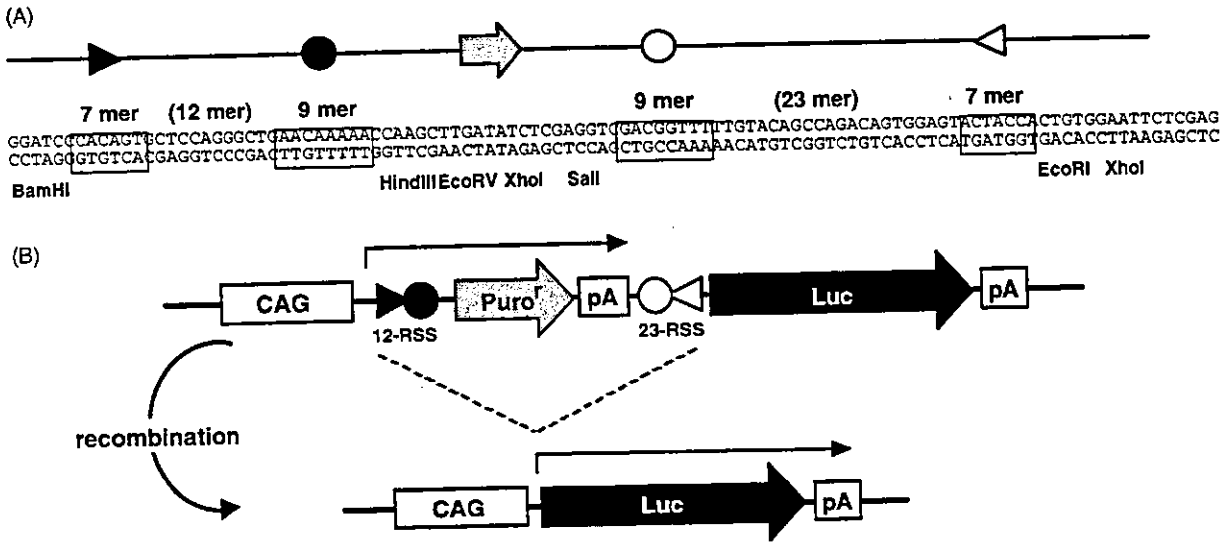

Fig. 2. Artificial recombination substrate used in this study. When RAG-dependent recombination occurs, the *puromycin*^{r} gene cassete flanked by two synthetic RSSs become deleted and the luciferase gene is relocated immediately downstream of the CAG promoter, leading to luciferase expression.

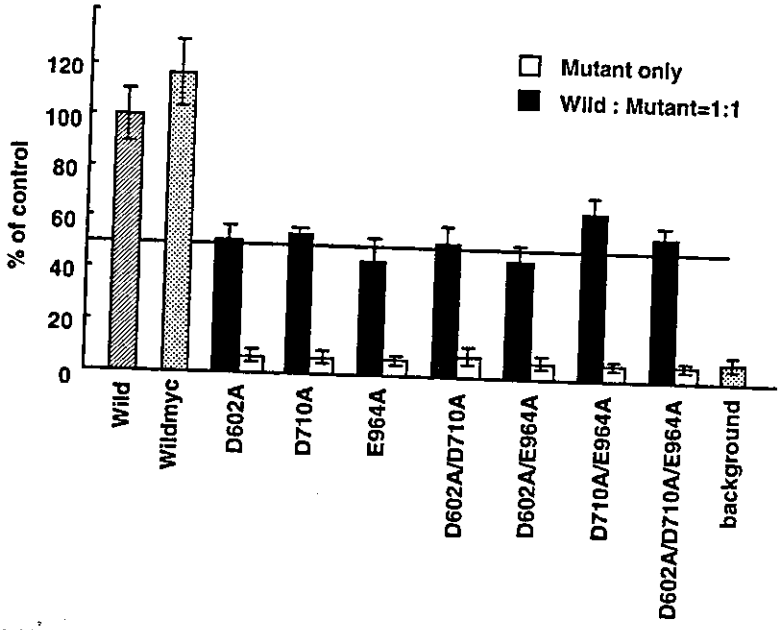

Fig. 3. Catalytic RAG1 mutants inhibit wild type RAG1. The recombination frequency is shown as a percentage of the value of wild type (shaded bar) and data are means ± S.D. from three independent experiments.

tail biopsies. The transgenic mice were healthy and indistinguishable from their littermates. If the mutant RAG1 protein inhibited V(D)J recombination during the process of B lymphocyte maturation, the production of antibodies might decrease in transgenic mice. To test this idea, we measured serum IgM concentrations, because IgM is the first type of antibody produced by the humoral immune system and maternal IgMs are not transferred to pups, as are other types of immunogloblins. The mean serum IgM levels of transgenic mice was significantly lower than that of the non-transgenic littermates at 5 weeks of age (314.5 ± 81.6 versus 227.8 ± 56.6 μg/ml, respectively, Fig. 5A) and this lower level was sustained at least until 8 weeks (485.6 ± 130.3 versus 292.2 ± 76.4 μg/ml, respectively, Fig. 5B). One of these transgenic lineages, no. 4, produced viable litters and F1 mice inherited the *GFPmutRAG1* gene and also showed low serum IgM levels compared to their littermates (Fig. 5C).

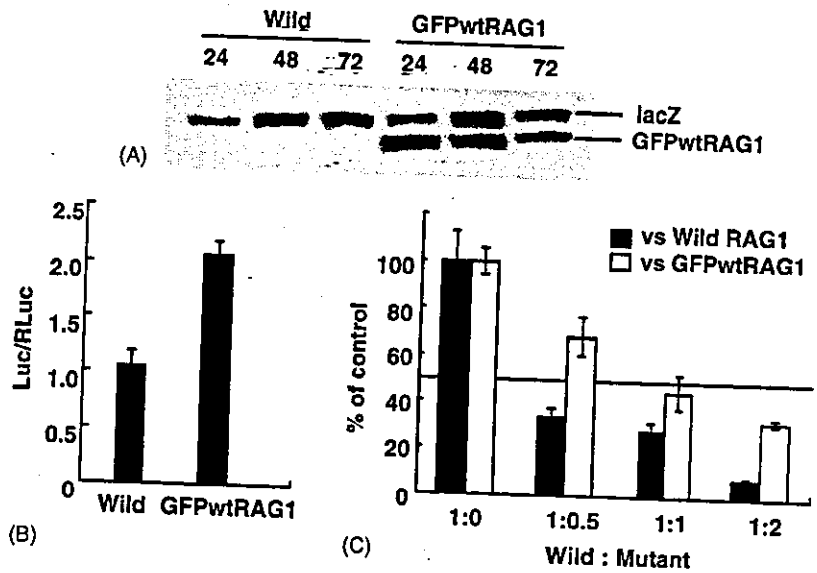

Fig. 4. (A) Protein expression of wild type RAG1 and GFPwtRAG1 obtained by transient expression in Cos7 cells. Fifty micrograms of total protein were electrophoresed per lane and the protein was detected with anti-myc antibody. (B) Recombination activty of GFPwtRAG1. Recombination frequency is shown as firefly lucifererase activity values normalized to *Renilla* luciferase activity. Data are means ± S.D. from three independent experiments. (C) Inhibition activity of GFPmutRAG1 against wild type RAG1 (solid bar) and GFPwtRAG1 (open bar). Data are means ± S.D. from three independent experiments.